

UCLA

UCLA Previously Published Works

Title

Remote Ischemic Conditioning Alters Methylation and Expression of Cell Cycle Genes in Aneurysmal Subarachnoid Hemorrhage

Permalink

<https://escholarship.org/uc/item/7tv2c5qv>

Journal

Stroke, 46(9)

ISSN

0039-2499

Authors

Nikkola, Elina
Laiwalla, Azim
Ko, Arthur
et al.

Publication Date

2015-09-01

DOI

10.1161/strokeaha.115.009618

Peer reviewed

Remote Ischemic Conditioning Alters Methylation and Expression of Cell Cycle Genes in Aneurysmal Subarachnoid Hemorrhage

Elina Nikkola, BS; Azim Laiwalla, MS; Arthur Ko, BS; Marcus Alvarez, BS; Mark Connolly, BS; Yinn Cher Ooi, MD; William Hsu, PhD; Alex Bui, PhD; Päivi Pajukanta, MD, PhD; Nestor R. Gonzalez, MD

Background and Purpose—Remote ischemic conditioning (RIC) is a phenomenon in which short periods of nonfatal ischemia in 1 tissue confers protection to distant tissues. Here we performed a longitudinal human pilot study in patients with aneurysmal subarachnoid hemorrhage undergoing RIC by limb ischemia to compare changes in DNA methylation and transcriptome profiles before and after RIC.

Methods—Thirteen patients underwent 4 RIC sessions over 2 to 12 days after rupture of an intracranial aneurysm. We analyzed whole blood transcriptomes using RNA sequencing and genome-wide DNA methylomes using reduced representation bisulfite sequencing, both before and after RIC. We tested differential expression and differential methylation using an intraindividual paired study design and then overlapped the differential expression and differential methylation results for analyses of functional categories and protein–protein interactions.

Results—We observed 164 differential expression genes and 3493 differential methylation CpG sites after RIC, of which 204 CpG sites overlapped with 103 genes, enriched for pathways of cell cycle ($P<3.8\times10^{-4}$) and inflammatory responses ($P<1.4\times10^{-4}$). The cell cycle pathway genes form a significant protein–protein interaction network of tightly coexpressed genes ($P<0.00001$).

Conclusions—Gene expression and DNA methylation changes in aneurysmal subarachnoid hemorrhage patients undergoing RIC are involved in coordinated cell cycle and inflammatory responses. (*Stroke*. 2015;46:2445–2451.)

DOI: 10.1161/STROKEAHA.115.009618

Key Words: aneurysm ■ DNA methylation ■ genomics ■ preconditioning
■ subarachnoid hemorrhage ■ transcriptome

Remote ischemic conditioning (RIC) is a phenomenon where nonlethal ischemic exposure in a peripheral tissue induces a systemic protection of subsequent injuries in distant organs and tissues.¹ RIC has shown encouraging results in animal models by providing cardio- and neuroprotective effects against an ischemic injury, and thus RIC is emerging as an attractive novel therapeutic for clinical trials.^{2–4} Recent human studies have confirmed the safety and feasibility of lower limb RIC in patients with aneurysmal subarachnoid hemorrhage (aSAH).^{5,6} Based on our separate study (Laiwalla et al, unpublished data), the odds ratio of a good outcome for patients with RIC is 5.17 (95% confidence interval, 1.21–25.02) when compared with matched controls with SAH.

The effectiveness of RIC is likely to be caused by its multifactorial effects, and rodent studies suggest that these are

mediated in part by a cascade of transcriptional and translational changes.⁷ Activation of basic cell survival responses to transient ischemia causes a shift toward a protective genetic profile, leading to a differential regulation of genes involved in inflammation, neurotransmitter excitotoxicity, apoptosis, and cerebrovascular perfusion.^{8–13} Nevertheless, the mechanisms by which RIC provides neuroprotective effects in human are not well understood. The involvement of humoral factors has been demonstrated in animals because the protection can be transferred from an RIC animal to a nonconditioned animal by whole blood transfusion.¹⁴ Thus, genetic and epigenetic studies in human blood could elucidate the humeral processes catalyzed by RIC and furthermore provide potential diagnostic and therapeutic targets for the treatment and prevention of ischemic injury.

Received March 31, 2015; final revision received June 11, 2015; accepted July 2, 2015.

From the Department of Human Genetics (E.N., A.K., M.A., P.P.), Department of Neurosurgery (A.L., M.C., Y.C.O., N.R.G.), and Department of Radiological Sciences (W.H., A.B., N.R.G.), David Geffen School of Medicine at UCLA, Los Angeles, CA; and Department of Human Genetics and Molecular Biology, Molecular Biology Institute at UCLA, Los Angeles, CA (A.K., P.P.).

The online-only Data Supplement is available with this article at <http://stroke.ahajournals.org/lookup/suppl/doi:10.1161/STROKEAHA.115.009618/-DC1>.

Correspondence to Nestor R. Gonzalez, MD, Associate Professor of Neurosurgery and Radiology, David Geffen School of Medicine at UCLA, 300 Stein Plaza, Suite 539, Los Angeles, CA 90095. E-mail nngonzalez@mednet.ucla.edu

© 2015 American Heart Association, Inc.

Stroke is available at <http://stroke.ahajournals.org>

DOI: 10.1161/STROKEAHA.115.009618

In this human pilot study, we performed a prospective longitudinal evaluation in a group of patients with aSAH undergoing RIC to study the induced genomic responses by identifying and comparing blood DNA methylation and gene expression profiles before RIC and 1 week after RIC. Identification of factors altered by a transient limb RIC can provide insights into the mechanisms of neuroprotective action and, ultimately, may yield biomarkers for SAH prognosis and treatment.

Methods

Study Samples

Patients with aSAH were enrolled from the Remote Ischemic Preconditioning in Subarachnoid Hemorrhage Trial (Clinicaltrials.gov No. NCT01158508). The study was approved by the local institutional review board, and all participants gave a written informed consent. Patients 18 to 80 years old with SAH confirmed by computed tomography or lumbar puncture and presence of a ruptured intracranial aneurysm confirmed by computed tomography, magnetic resonance, or catheter angiography were considered for enrollment in this study. Patients who were pregnant or with a history or physical examination findings of peripheral vascular disease, deep venous thrombosis, peripheral neuropathy, or lower extremity bypass were excluded. Clinical characteristics are provided in Table 1.

RIC Protocol

Patients underwent 4 RIC sessions over 2 to 12 days after aneurysm rupture. RIC sessions were performed on the lower limb with a large adult-sized blood pressure cuff. Each session consisted of 4 inflation cycles lasting 5 minutes, followed by 5-minute deflations. Cuff pressure was originally inflated at 20 mm Hg over the patient's baseline systolic blood pressure, then increased until the dorsalis pedis pulse was abolished, as confirmed by a Doppler ultrasonography. This pressure was maintained for 5 minutes throughout the duration of the inflation cycle.

Peripheral blood samples were drawn from aSAH patients at 2 different time points: before RIC (baseline) and after 4 sessions of the RIC treatment. DNA and RNA were isolated according to standard protocols.

Aneurysm Controls

We included 24 control individuals with a history of intracranial aneurysms who never received RIC treatment. The blood collection and

sample processing were performed in the same way as described for the aSAH cases above.

RNA Sequencing

We included 13 aSAH sample pairs and 24 aneurysm controls in the study after the initial quality control of the blood RNA (RNA integrity number [RIN] value >7, RNA concentration >10 ng/μL). The blood RNA sequencing libraries were prepared using Illumina TruSeq RNA library kit, and sequencing of the paired-end, 100-bp reads was performed using the Illumina HiSeq2000 platform, resulting in on average 46.1 mol/L reads per sample. We used STAR¹⁵ to align the fastq files to the human GRCh37/hg19 reference genome with the following settings: the maximum intron size was set at 500 kb; the minimum intron size was set at 20; and we allowed for 4 mismatches. We used HTSeq (version HTSeq-0.6.1)¹⁶ to produce raw counts.

Differential Expression Using EdgeR and DESeq2

We used both EdgeR¹⁷ and DESeq2¹⁸ R-packages to identify differentially expressed (DE) genes using the paired sample design and focused on their overlap to obtain a set of highly confident DE genes. First, using EdgeR, we excluded the genes that did not have one count per million reads in at least 50% of the samples. We normalized the read count values using trimmed means of *M* value and estimated common, trended, and tagwise dispersions using R software (version RX64 3.0.2). Together, these quality control steps removed genes with low expression and normalized the libraries for library size and biological variability, resulting in 14 816 genes for our subsequent analyses. We determined DE using the generalized linear model likelihood ratio test using a significance threshold of FDR <0.05.

Second, similarly as in EdgeR, we used a multifactor design with DESeq2. We estimated the size factors and dispersions and performed negative binomial generalized linear model fitting for the sample as a factor and Wald statistics for DE. We used Benjamini–Hochberg-adjusted *P*<0.05 as a threshold for significance.

To compare the aSAH patients with aneurysm controls, we considered only the genes DE between the aSAH baseline and after the treatment. We performed 2 separate DE analyses using negative binomial and determined DE using Wald test for (1) the aSAH baseline group versus the controls and (2) the aSAH RIC treatment group versus the controls (Figure I in the online-only Data Supplement). The genes changing the DE status between the 2 analyses (ie, the genes that were not DE between the aSAH baseline group and controls, but became DE when comparing the

Table 1. Clinical Characteristics of the aSAH Patients

Subject ID	Age	Sex	Smoking	Alcohol	Hypertension	T2D	Vasospasm	Clinical Functional Outcome
SAH 551	61	F	No	No	No	No	N	Improved or no change
SAH 553	77	F	No	No	No	No	Y	Improved or no change
SAH 554	56	M	Former	No	No	No	Y	Improved or no change
SAH 555	53	F	No	No	No	No	Y	Deteriorated
SAH 556	23	F	No	No	No	No	N	Improved or no change
SAH 557	47	F	No	No	Yes	No	Y	Deteriorated
SAH 558	65	F	No	No	Yes	No	Minimal	Improved or no change
SAH 559	43	F	Yes	Yes	Yes	No	Y	Improved or no change
SAH 5510	36	M	Yes	Yes	No	No	Y	Improved or no change
SAH 5511	51	M	Yes	Yes	Yes	Yes	N	Improved or no change
SAH 5512	43	M	Yes	No	Yes	Yes	Y	Improved or no change
SAH 5513	60	F	No	No	Yes	Yes	Y	Deteriorated
SAH 5514	51	M	Yes	Yes	Yes	No	Suspected	Improved or no change

SAH indicates subarachnoid hemorrhage; and T2D, type 2 diabetes mellitus.

aSAH treatment group with the controls) were carried forward to subsequent analyses.

Methylation

We analyzed blood DNA methylation profiles by reduced representation bisulfite sequencing (RRBS). RRBS libraries from human genomic DNA were prepared as previously described.¹⁹ Briefly, we treated blood DNA with sodium bisulfite (Epitech Illumina), digested it with the MspI enzyme, and selected fragments averaging 100 to 250 bp. We multiplexed 4 samples per lane and sequenced the libraries using single-end 100-bp reads with the Illumina Hiseq2000 platform, resulting in on average 25.1 mol/L reads per sample.

We performed initial QC for fastq files using FastaQC. We used BS-seeker²⁰ with Bowtie2²¹ for RRBS alignment using hg19 as a reference genome. For alignment, we considered in silico MspI fragments between 40 and 500 bp to cover all possible MspI fragments from the RRBS libraries. We aligned the reads using the Bowtie2 end-to-end alignment mode by allowing 4 mismatches. We called the methylation status of the individual CpG sites (percentage of methylated cells) by requiring at least 10 reads per a CpG site. Pearson correlation coefficient was used to estimate pair-wise correlations in methylation sites between the individuals. Paired Students *t*-tests were conducted to compare between-group and within-group differences. The CpG sites passing a 2-tailed nominal $P<0.01$ were considered significant and carried forward for subsequent analyses. Finally, we used BEDTOOLS²² to overlap the DE genes with methylated regions.

Functional Annotation and Coexpression of the Pathway Genes

We used DAVID software^{23,24} to search for functional categories of the DE genes. To highlight the most relevant gene ontology terms associated with the overlapped DE and differential methylation (DM) gene lists, we performed a batch annotation and gene-GO term enrichment analysis. We searched for protein–protein interaction (PPI) networks using STRING v9.1.²⁵ We used Pearson correlation coefficient to estimate correlations between the pathway genes and ggplot2 and reshape2 to visualize these results. Reactome^{26,27} was used to explore specific pathways.

Results

The overall study design is shown in Figure 1. To identify genomic mechanisms for the effects of RIC in aSAH patients, we used a paired sample design where each patient gave blood samples before and after 4 RIC sessions. Using this longitudinal study design, each individual functions as a control for him-/herself in the DE and DM analyses. Accordingly, we

were able to adjust for potential confounding factors, such as age, smoking, medication, and ethnicity, using this intra-individual paired design. We analyzed the blood RNA expression and DNA methylation profiles of each patient before RIC and 1 week after the RIC treatment started. We compared these profiles to the ones of the controls who did not receive any RIC treatments. Finally, we overlapped the DE genes with DM sites and performed functional annotations and PPIs analysis of the overlapping genes (Figure 1).

Differential Expression

We found 451 DE genes after RIC ($FDR<0.05$) consistently using both EdgeR and DESeq2, of which 205 were upregulated after the RIC treatment and 246 were downregulated, respectively (Figure 2; and Table I in the online-only Data Supplement). Next, to identify genes responding to the RIC treatment, we tested the expression of the 451 genes in the controls for DE against their expression at both the aSAH baseline and after the RIC treatment, considering a Bonferroni-corrected $P<1.1\times 10^{-4}$ ($P<0.05/451$ DE genes) significant. We found 164 DE genes (see Table II in the online-only Data Supplement for the list of DE genes) between the controls and aSAH patients before and after RIC treatment, suggesting that these genes may contribute to the response to the RIC treatment.

Differential Methylation

We were able to map on average 66% of reads/sample to the human genome, which is in accordance with previous RRBS studies.^{20,28} The resulting methylation profiles per sample covered on average 1764402 CpG sites, of which 676543 were assayed in all individuals. The overall methylation status changed little within an individual ($\approx 98\%$) and between individuals ($\approx 97.5\%$; Figure II in the online-only Data Supplement), suggesting that methylation is a stable phenomenon and only a small number of sites are actively responding to environmental factors. We focused on the 403546 CpG sites that altered by $>10\%$ in at least one individual after RIC. To test DM cytosines between the baseline and after treatment, we used 2-tailed paired student's *t* test. A total of 3493 CpG sites were DM ($P<0.01$).

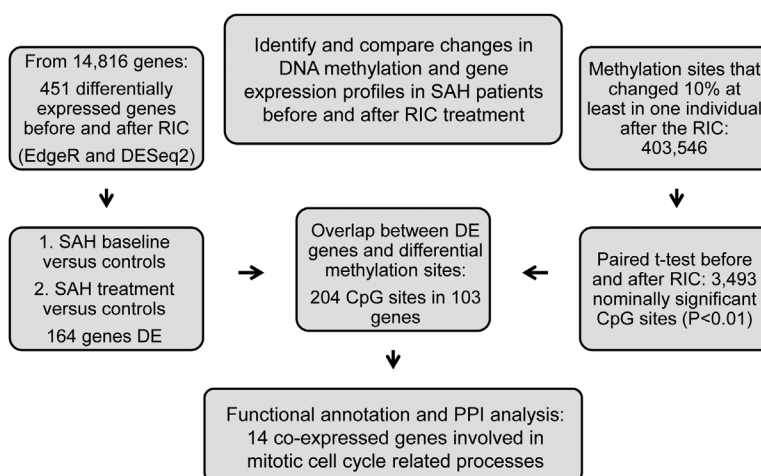


Figure 1. A schematic overview of study design and results. DE indicates differential expression; PPI, protein–protein interaction; RIC, remote ischemic conditioning; and SAH, subarachnoid hemorrhage.

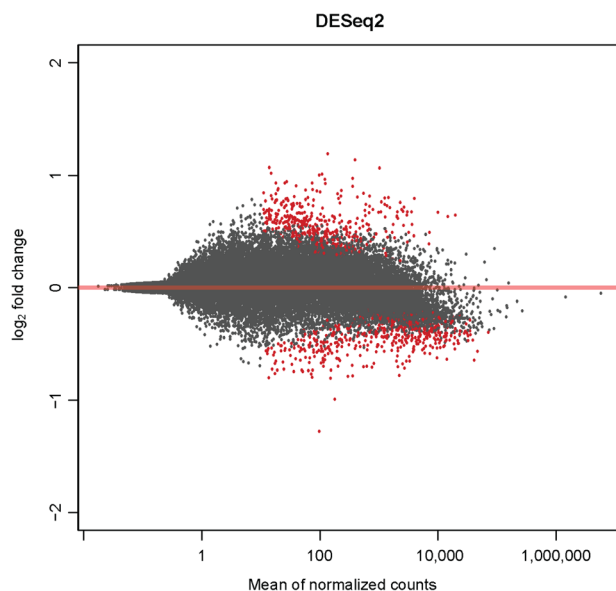


Figure 2. The differentially expressed (DE) genes between the aneurysmal subarachnoid hemorrhage (aSAH) baseline and a week after remote ischemic conditioning (RIC) treatment. Red dots indicate DE genes with an FDR <0.05.

Overlapping the DE and DM Regions

When we overlapped (defined ± 250 kb from the each DE gene) the DM CpGs with the DE genes, we found 204 CpG sites corresponding to 103 DE and DM genes, suggesting methylation as a potential mechanism for DE (Table III in the online-only Data Supplement). Furthermore, 52 of the genes had >1 nearby DM site.

Functional Annotation and Coexpression of the Pathway Genes

Functional annotation with DAVID software showed that the overlapping 103 DE and DM genes are enriched for defense and inflammatory responses (Benjamini–Hochberg [B-H]–corrected $P<1.4\times 10^{-4}$) and for cell cycle and mitosis (B-H–corrected $P<3.8\times 10^{-4}$; Table 2). In addition, we examined the PPIs of the 103 DE genes using String (Figure 3). We found a

Table 2. Functional Annotations of the 103 Identified DE Genes Using the David Pathway Tool

	Gene Count	B-H Corrected P Value
Enrichment score 4.35		
Cluster 1		
Defense response	18	1.4×10^{-4}
Inflammatory response	10	1.7×10^{-2}
Enrichment score 3.95		
Cluster 2		
Cell cycle	19	3.8×10^{-4}
M phase	12	1.7×10^{-3}
Cell cycle phase	13	1.9×10^{-3}
Nuclear division	10	1.7×10^{-3}
Mitosis	10	1.7×10^{-3}

B-H indicates P value after Benjamini–Hochberg correction for false discovery rate; and DE, differential expression.

significant enrichment for PPIs and one large network consisting of 21 DE and DM genes (Figure 3), of which 14 are part of the cell cycle pathway from the functional enrichment analysis (Table 2). We also found 2 smaller PPIs consisting of 3 proteins each: *CEBPB*, *HDAC4*, *PPARG* and *AZU1*, *CTSG*, *MPO* (Figure 3), all present in the significant pathways of defense and inflammatory response mechanisms (Table 2).

Next, we further examined the 14 cell cycle pathway genes for correlations between their gene expressions. These genes exhibited highly dynamic correlation shifts, with substantially tighter correlations after the RIC treatment (Figure 4), suggesting that different phases of cell cycle pathway are turned on as a result of RIC. Interestingly, when we visualized the coexpression of these genes in the control group, we observed a clear difference in their correlations when compared with the aSAH patients at baseline and even more after the treatment (Figure 4), indicating the involvement of these genes in aSAH and the potential influence of the RIC treatment.

Based on a more detailed Reactome pathway analysis (Table IV in the online-only Data Supplement), 8 of the 14 genes ($FDR<1.0\times 10^{-5}$) are involved in the cell cycle pathway (*SPC24*, *ESPL1*, *CLSPN*, *CDC45*, *CENPF*, *FOXM1*, *CDK1*, *RAD51*). In the Reactome analysis, *CDK1* acts as a key regulator of specific mitotic cell cycle pathways. For instance, we observed that *CDK1* is involved in G2/M transition and mitotic G2-G2/M phases with *CENPF* and *FOXM1*, regulating the G2/M checkpoints with *CLSPN* and *CDC45*. In addition, *CDK1* is involved in processes such as kinetochore assembly in mitotic prometaphase and M Phase with *SPC24*, *CENPF*, and *ESPL1* (Table IV in the online-only Data Supplement). *CDK1* is also present in numerous activation and signaling pathways within mitotic cell cycle pathway (Table IV in the online-only Data Supplement).

Discussion

We performed the first longitudinal and systematic genome-wide pilot study in humans comparing gene expression and methylation changes after RIC in aSAH. We found 164 DE genes and 3493 DM CpG sites that are modified, potentially as a result of RIC. When we overlapped these regions, we observed 204 DM CpG sites corresponding to 103 DE genes, suggesting methylation as a potential mechanism regulating gene expression. These genes were enriched for cell cycle–related processes, as well as for defense and inflammatory responses. Furthermore, the identified 14 cell cycle genes exhibited highly correlated expression signals after RIC (Figure 4). Overall, these findings provide first insights into the neuroprotective molecular mechanisms underlying RIC in humans.

Our prior work has demonstrated RIC-induced metabolic changes in the preconditioned limb, as well as cerebral tissue.^{29,30} Muscle microdialysis during RIC showed an increase in lactate/pyruvate ratio and lactate, without change in glycerol.²⁹ Cerebral microdialysis during RIC showed a decrease in lactate/pyruvate ratio and glycerol, which persisted after the last RIC session.³⁰ Identification of markers of the RIC effects beyond local factors is imperative for determining appropriate end points in future RIC clinical studies.

Whole-genome transcriptional analysis has been applied to uncover genetic changes underlying ischemia-induced

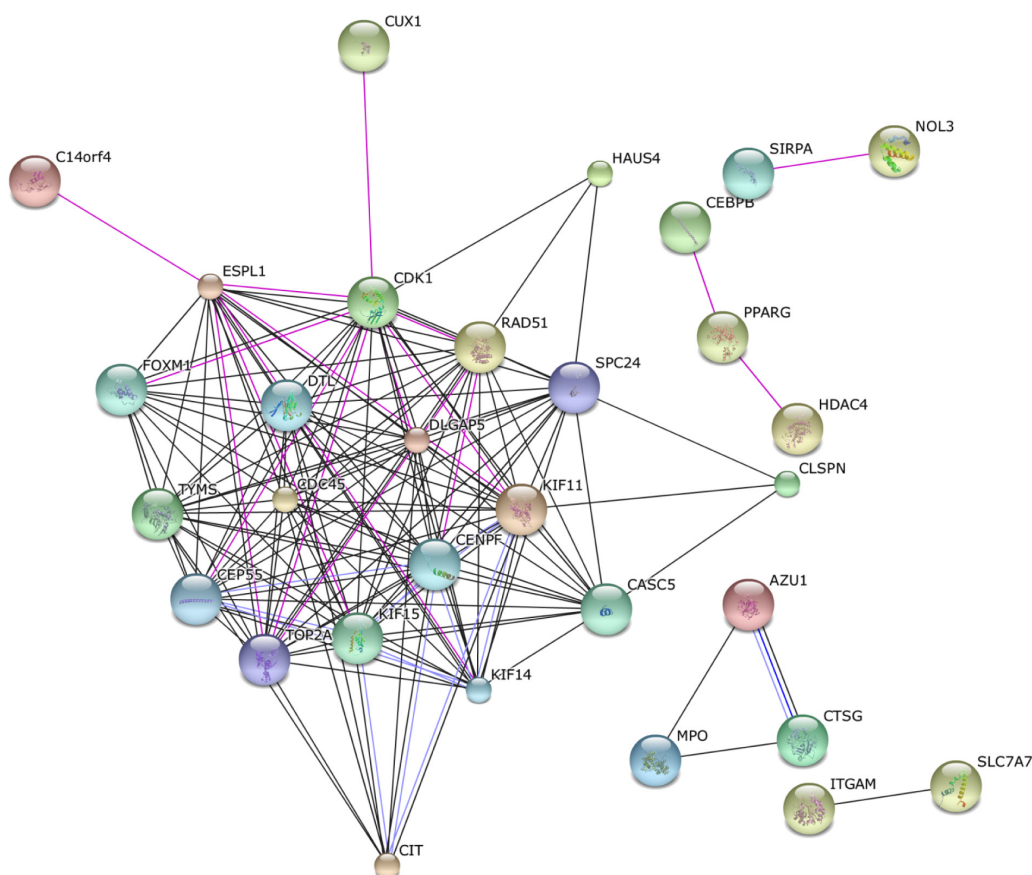


Figure 3. Protein–protein interactions (PPIs) of the 103 differentially expressed (DE) genes using String. We observed a statistically significant ($P<0.00001$) enrichment of PPIs of the DE genes residing in the cell cycle, defense, and inflammatory response pathways, all passing the Benjamini correction as shown in Table 2.

neuroprotective effects in animal models.^{31,32} DNA methylation changes of gene promoter regions have also been investigated to uncover preconditioning-induced epigenetic changes, contributing to neuroprotection in mice.³³ Although proof of concept animal studies have given great insight into the potential mechanisms of RIC, they do not necessarily translate directly to humans, and thus, human studies are essential to evaluate effects in clinical settings.

Cell cycle machinery and related molecules have been previously implicated in ischemic neuronal death,^{34,35} and

irregular cell cycle activation has been implicated in stroke.^{36–38} We show evidence for involvement of genes in cell cycle processes regulated by *CDK1* in the acute stage of aSAH, possibly modified by RIC (Figure 4). We postulate that this pathway may be important in various forms of ischemia. Furthermore, we hypothesize that RIC may induce a release of substances from the ischemic limb muscles to blood. These in turn stimulate white blood cells, such as macrophages, to increase the expression of genes involved in cell cycle and cell proliferation. Subsequently, these white blood cells may stream to the

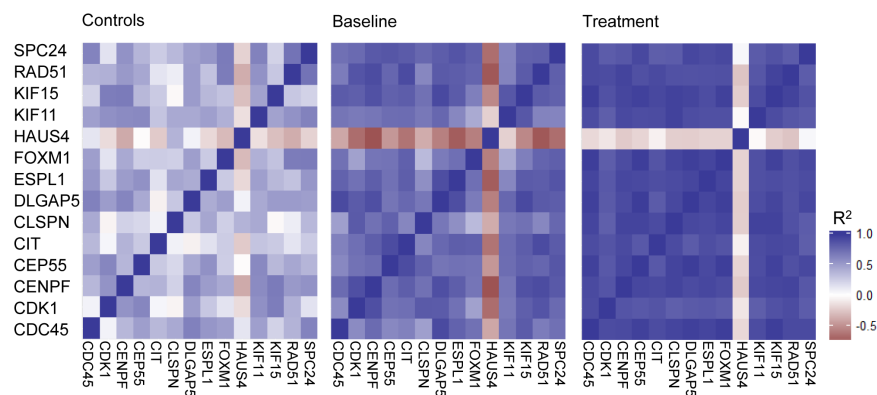


Figure 4. Co-expression analysis of the 14 mitotic cell cycle genes identified in the Protein–protein interactions (PPIs) and functional enrichment analyses.

ischemic location in brain and release substances, including growth factors and other cytokines, to protect brain from further apoptosis. This mechanism could lead to the neuroprotective effects of RIC, although additional functional studies are warranted to verify the underlying mechanisms.

One of the mechanisms proposed for RIC is inflammatory responses.^{39,40} In accordance with this, our DAVID pathway analysis implicated a set of 18 both DE and DM genes in defense response pathways (*CEPB*, *AZU1*, *BPI*, *CTSG*, *CRISP3*, *CYSLTR1*, *HDAC4*, *INHBA*, *IL1R1*, *IL10RB*, *LTF*, *MPO*, *OLR1*, *PPARG*, *PROK2*, *STAT5B*, *STAB1*, and *TLR5*). Six of these genes were also involved in 2 separate PPIs (Figure 3).

A recent study exploring human plasma proteome in RIC found that cysteine-rich secretory protein 3 (CRISP-3) was increased in serum after RIC in 6 adults.⁴¹ This is consistent with our finding of over a 2-fold increase of *CRISP3* gene expression in blood followed by RIC (Table I in the online-only Data Supplement), suggesting its role as a humoral RIC mediator and surrogate marker. CRISP-3 is a glycoprotein present in exocrine secretions, bone marrow, secretory granules of neutrophils, and plasma bound to a1B glycoprotein.^{42,43} Although its complete function is unknown, it is thought to act in innate immune response and as a prostate cancer marker.^{42,43}

In summary, in this first pilot study, using a longitudinal design to investigate genome-wide expression and methylation changes in aSAH patients after RIC, we found evidence for coordinated expression and methylation changes of a small set of key genes in mitotic cell cycle, defense, and inflammatory responses. We have limitations in this study, and therefore, the results presented here should be further investigated and verified in future considerably larger genomic studies. In addition to the small sample size, we recognize that some of the observed changes in genes expression and methylation are potentially because of other medical treatments these patients received in the hospital, and hence, future studies should comprise a randomization that includes patients not receiving any RIC treatment as controls. We also recognize that differences in blood cell types may contribute to the changes in DNA methylation and gene expression, and thus future RIC studies should include analysis of separate fluorescence activated cell sorting-sorted cells. Nevertheless, longitudinal genome-wide studies of stroke, and especially SAH, integrating expression and methylation changes at the genome-wide level are still sparse, and thus our study provides valuable initial data, starting to elucidate the largely unknown mechanisms underlying RIC in humans.

Sources of Funding

This work was supported by the Ruth and Raymond Stotter Endowment, the National Institutes of Health National Institute of Neurological Disorders and Stroke (NINDS) grant K23NS079477, National Institute of Biomedical Imaging and Bioengineering (NIBIB) grant R01EB000362, and the National Heart, Lung, and Blood Institute (NHLBI) grants HL-28481 and HL-095056.

Disclosures

None.

References

- Przyklenk K, Bauer B, Ovize M, Kloner RA, Whittaker P. Regional ischemic 'preconditioning' protects remote virgin myocardium from subsequent sustained coronary occlusion. *Circulation*. 1993;87:893–899.
- Ren C, Gao X, Steinberg GK, Zhao H. Limb remote-preconditioning protects against focal ischemia in rats and contradicts the dogma of therapeutic time windows for preconditioning. *Neuroscience*. 2008;151:1099–1103. doi: 10.1016/j.neuroscience.2007.11.056.
- Li SJ, Wu YN, Kang Y, Yin YQ, Gao WZ, Liu YX, et al. Noninvasive limb ischemic preconditioning protects against myocardial I/R injury in rats. *J Surg Res*. 2010;164:162–168. doi: 10.1016/j.jss.2009.03.017.
- Wei D, Ren C, Chen X, Zhao H. The chronic protective effects of limb remote preconditioning and the underlying mechanisms involved in inflammatory factors in rat stroke. *PLoS One*. 2012;7:e30892. doi: 10.1371/journal.pone.0030892.
- Koch S, Katsnelson M, Dong C, Perez-Pinzon M. Remote ischemic limb preconditioning after subarachnoid hemorrhage: a phase Ib study of safety and feasibility. *Stroke*. 2011;42:1387–1391. doi: 10.1161/STROKEAHA.110.605840.
- Gonzalez NR, Connolly M, Dusick JR, Bhakta H, Vespa P. Phase I clinical trial for the feasibility and safety of remote ischemic conditioning for aneurysmal subarachnoid hemorrhage. *Neurosurgery*. 2014;75:590–598, discussion 598. doi: 10.1227/NEU.0000000000000514.
- Sarabi AS, Shen H, Wang Y, Hoffer BJ, Bäckman CM. Gene expression patterns in mouse cortical penumbra after focal ischemic brain injury and reperfusion. *J Neurosci Res*. 2008;86:2912–2924. doi: 10.1002/jnr.21734.
- Konstantinov IE, Arab S, Kharbanda RK, Li J, Cheung MM, Cherepanov V, et al. The remote ischemic preconditioning stimulus modifies inflammatory gene expression in humans. *Physiol Genomics*. 2004;19:143–150. doi: 10.1152/physiolgenomics.00046.2004.
- Zhang J, Qian H, Zhao P, Hong SS, Xia Y. Rapid hypoxia preconditioning protects cortical neurons from glutamate toxicity through delta-opioid receptor. *Stroke*. 2006;37:1094–1099. doi: 10.1161/01.STR.0000206444.29930.18.
- Liu YX, Zhang M, Liu LZ, Cui X, Hu YY, Li WB. The role of glutamate transporter-1a in the induction of brain ischemic tolerance in rats. *Glia*. 2012;60:112–124. doi: 10.1002/glia.21252.
- Ding ZM, Wu B, Zhang WQ, Lu XJ, Lin YC, Geng YJ, et al. Neuroprotective effects of ischemic preconditioning and postconditioning on global brain ischemia in rats through the same effect on inhibition of apoptosis. *Int J Mol Sci*. 2012;13:6089–6101. doi: 10.3390/ijms13056089.
- Zhang N, Yin Y, Han S, Jiang J, Yang W, Bu X, et al. Hypoxic preconditioning induced neuroprotection against cerebral ischemic injuries and its cPKC γ -mediated molecular mechanism. *Neurochem Int*. 2011;58:684–692. doi: 10.1016/j.neuint.2011.02.007.
- Nakamura H, Katsumata T, Nishiyama Y, Otori T, Katsura K, Katayama Y. Effect of ischemic preconditioning on cerebral blood flow after subsequent lethal ischemia in gerbils. *Life Sci*. 2006;78:1713–1719. doi: 10.1016/j.lfs.2005.08.008.
- Dickson EW, Reinhardt CP, Renzi FP, Becker RC, Porcaro WA, Heard SO. Ischemic preconditioning may be transferable via whole blood transfusion: preliminary evidence. *J Thromb Thrombolysis*. 1999;8:123–129.
- Dobin A, Davis CA, Schlesinger F, Drenkow J, Zaleski C, Jha S, et al. STAR: ultrafast universal RNA-seq aligner. *Bioinformatics*. 2013;29:15–21. doi: 10.1093/bioinformatics/bts635.
- Anders S, Pyl PT, Huber W. HTSeq—a Python framework to work with high-throughput sequencing data. *Bioinformatics*. 2015;31:166–169. doi: 10.1093/bioinformatics/btu638.
- Robinson MD, McCarthy DJ, Smyth GK. edgeR: a Bioconductor package for differential expression analysis of digital gene expression data. *Bioinformatics*. 2010;26:139–140. doi: 10.1093/bioinformatics/btp616.
- Love MI, Huber W, Anders S. Moderated estimation of fold change and dispersion for RNA-seq data with DESeq2. *Genome Biol*. 2014;15:550. doi: 10.1186/s13059-014-0550-8.
- Chen PY, Ganguly A, Rubbi L, Orozco LD, Morselli M, Ashraf D, et al. Intrauterine calorie restriction affects placental DNA methylation and gene expression. *Physiol Genomics*. 2013;45:565–576. doi: 10.1152/physiolgenomics.00034.2013.
- Guo W, Fiziev P, Yan W, Cokus S, Sun X, Zhang MQ, et al. BS-Seeker2: a versatile aligning pipeline for bisulfite sequencing data. *BMC Genomics*. 2013;14:774. doi: 10.1186/1471-2164-14-774.

21. Langmead B, Salzberg SL. Fast gapped-read alignment with Bowtie 2. *Nat Methods*. 2012;9:357–359. doi: 10.1038/nmeth.1923.
22. Quinlan AR, Hall IM. BEDTools: a flexible suite of utilities for comparing genomic features. *Bioinformatics*. 2010;26:841–842. doi: 10.1093/bioinformatics/btq033.
23. Huang da W, Sherman BT, Lempicki RA. Systematic and integrative analysis of large gene lists using DAVID bioinformatics resources. *Nat Protoc*. 2009;4:44–57. doi: 10.1038/nprot.2008.211.
24. Huang da W, Sherman BT, Lempicki RA. Bioinformatics enrichment tools: paths toward the comprehensive functional analysis of large gene lists. *Nucleic Acids Res*. 2009;37:1–13. doi: 10.1093/nar/gkn923.
25. Franceschini A, Szklarczyk D, Frankild S, Kuhn M, Simonovic M, Roth A, et al. STRING v9.1: protein–protein interaction networks, with increased coverage and integration. *Nucleic Acids Res*. 2013;41(Database issue):D808–D815. doi: 10.1093/nar/gks1094.
26. Milacic M, Haw R, Rothfels K, Wu G, Croft D, Hermjakob H, et al. Annotating cancer variants and anti-cancer therapeutics in reactome. *Cancers (Basel)*. 2012;4:1180–1211. doi: 10.3390/cancers4041180.
27. Croft D, Mundo AF, Haw R, Milacic M, Weiser J, Wu G, et al. The Reactome pathway knowledgebase. *Nucleic Acids Res*. 2014;42(Database issue):D472–D477. doi: 10.1093/nar/gkt1102.
28. Doherty R, Couldrey C. Exploring genome wide bisulfite sequencing for DNA methylation analysis in livestock: a technical assessment. *Front Genet*. 2014;5:126. doi: 10.3389/fgene.2014.00126.
29. Bilgin-Freiert A, Dusick JR, Stein NR, Etchepare M, Vespa P, Gonzalez NR. Muscle microdialysis to confirm sublethal ischemia in the induction of remote ischemic preconditioning. *Transl Stroke Res*. 2012;3:266–272. doi: 10.1007/s12975-012-0153-1.
30. Gonzalez NR, Hamilton R, Bilgin-Freiert A, Dusick J, Vespa P, Hu X, et al. Cerebral hemodynamic and metabolic effects of remote ischemic preconditioning in patients with subarachnoid hemorrhage. *Acta Neurochir Suppl*. 2013;115:193–198. doi: 10.1007/978-3-7091-1192-5_36.
31. Stenzel-Poore MP, Stevens SL, Xiong Z, Lessov NS, Harrington CA, Mori M, et al. Effect of ischaemic preconditioning on genomic response to cerebral ischaemia: similarity to neuroprotective strategies in hibernation and hypoxia-tolerant states. *Lancet*. 2003;362:1028–1037. doi: 10.1016/S0140-6736(03)14412-1.
32. Stenzel-Poore MP, Stevens SL, Simon RP. Genomics of preconditioning. *Stroke*. 2004;35(11 suppl 1):2683–2686. doi: 10.1161/01.STR.0000143735.89281.bb.
33. Zhang S, Zhang Y, Jiang S, Liu Y, Huang L, Zhang T, et al. The effect of hypoxia preconditioning on DNA methyltransferase and PP1 γ in hippocampus of hypoxia preconditioned mice. *High Alt Med Biol*. 2014;15:483–490. doi: 10.1089/ham.2014.1042.
34. Rashidian J, Iyirhiaro GO, Park DS. Cell cycle machinery and stroke. *Biochim Biophys Acta*. 2007;1772:484–493. doi: 10.1016/j.bbadi.2006.11.009.
35. Wang W, Bu B, Xie M, Zhang M, Yu Z, Tao D. Neural cell cycle dysregulation and central nervous system diseases. *Prog Neurobiol*. 2009;89:1–17. doi: 10.1016/j.pneurobio.2009.01.007.
36. Osuga H, Osuga S, Wang F, Fetni R, Hogan MJ, Slack RS, et al. Cyclin-dependent kinases as a therapeutic target for stroke. *Proc Natl Acad Sci U S A*. 2000;97:10254–10259. doi: 10.1073/pnas.170144197.
37. Wang F, Corbett D, Osuga H, Osuga S, Ikeda JE, Slack RS, et al. Inhibition of cyclin-dependent kinases improves CA1 neuronal survival and behavioral performance after global ischemia in the rat. *J Cereb Blood Flow Metab*. 2002;22:171–182. doi: 10.1097/00004647-200202000-00005.
38. Rashidian J, Iyirhiaro G, Aleyasin H, Rios M, Vincent I, Callaghan S, et al. Multiple cyclin-dependent kinases signals are critical mediators of ischemia/hypoxic neuronal death *in vitro* and *in vivo*. *Proc Natl Acad Sci U S A*. 2005;102:14080–14085. doi: 10.1073/pnas.0500099102.
39. Bowen KK, Naylor M, Vemuganti R. Prevention of inflammation is a mechanism of preconditioning-induced neuroprotection against focal cerebral ischemia. *Neurochem Int*. 2006;49:127–135. doi: 10.1016/j.neuint.2006.02.011.
40. Carr-White G, Koh T, DeSouza A, Haxby E, Kemp M, Hooper J, et al. Chronic stable ischaemia protects against myocyte damage during beating heart coronary surgery. *Eur J Cardiothorac Surg*. 2004;25:772–778. doi: 10.1016/j.ejcts.2004.02.011.
41. Helgeland E, Breivik LE, Vaudel M, Svendsen ØS, Garberg H, Nordrehaug JE, et al. Exploring the human plasma proteome for humoral mediators of remote ischemic preconditioning—a word of caution. *PLoS One*. 2014;9:e109279. doi: 10.1371/journal.pone.0109279.
42. Elias MF, Zainal Ariffin SH, Karsani SA, Abdul Rahman M, Senafi S, Megat Abdul Wahab R. Proteomic analysis of saliva identifies potential biomarkers for orthodontic tooth movement. *ScientificWorldJournal*. 2012;2012:647240. doi: 10.1100/2012/647240.
43. Udby L, Sørensen OE, Pass J, Johnsen AH, Behrendt N, Borregaard N, et al. Cysteine-rich secretory protein 3 is a ligand of alpha1B-glycoprotein in human plasma. *Biochemistry*. 2004;43:12877–12886. doi: 10.1021/bi048823e.

ONLINE SUPPLEMENT

Remote Ischemic Conditioning Alters Methylation and Expression of Cell Cycle Genes in Aneurysmal Subarachnoid Hemorrhage

Elina Nikkola, Azim Laiwalla, Arthur Ko, Marcus Alvarez, Mark Connolly, Yinn Cher Ooi,
William Hsu, Alex Bui, Päivi Pajukanta, and Nestor Gonzalez

Supplemental Tables

Table I. The 451 differentially expressed genes passing FDR<0.05. The results shown here are from DESeq2 R-package.

Gene	Mean	log2FC	Stat	B-H Adjusted p-value
HTRA1	98	-1.28	-6.73	2.47x10 ⁻⁷
MYB	121	0.96	6.23	3.38x10 ⁻⁶
HRH4	123	0.92	5.98	1.09x10 ⁻⁵
MAK	621	-0.70	-5.93	1.10x10 ⁻⁵
MYO7A	177	-1.00	-5.80	1.61x10 ⁻⁵
OLR1	136	1.19	5.82	1.61x10 ⁻⁵
CRISP3	394	1.13	5.66	2.93x10 ⁻⁵
FBN1	27	0.94	5.65	2.93x10 ⁻⁵
CD52	2032	0.63	5.33	1.46x10 ⁻⁴
RSAD2	1025	1.07	5.19	2.68x10 ⁻⁴
SERPINB10	108	1.01	5.13	3.24x10 ⁻⁴
STAT5B	13869	-0.43	-5.04	4.74x10 ⁻⁴
SUFU	566	-0.41	-5.04	4.74x10 ⁻⁴
MRVI1	2714	-0.72	-5.00	5.38x10 ⁻⁴
BCL2L15	74	0.93	4.95	6.44x10 ⁻⁴
SSH1	2477	-0.49	-4.92	7.15x10 ⁻⁴
IDO1	98	1.00	4.88	8.44x10 ⁻⁴
ANLN	39	0.91	4.85	8.96x10 ⁻⁴
DNAH17	1640	-0.56	-4.85	8.96x10 ⁻⁴
TGFBI	3328	-0.66	-4.83	9.26x10 ⁻⁴
HAUS4	1226	-0.57	-4.80	9.70x10 ⁻⁴
RP11-473M20.5	362	-0.79	-4.81	9.70x10 ⁻⁴
MANSC1	2500	-0.68	-4.78	1.03x10 ⁻³
MS4A3	355	0.97	4.76	1.12x10 ⁻³
RP5-968J1.1	49	-0.73	-4.75	1.15x10 ⁻³
ETS2	2895	-0.65	-4.72	1.20x10 ⁻³
P2RY14	230	0.86	4.72	1.20x10 ⁻³
ATP2B4	3792	-0.57	-4.69	1.36x10 ⁻³
BRIP1	26	0.79	4.66	1.52x10 ⁻³
CD163	2193	-0.78	-4.60	1.97x10 ⁻³
ACSL1	40710	-0.65	-4.58	2.14x10 ⁻³
RP11-1D12.2	26	0.93	4.57	2.19x10 ⁻³
FAM129A	19351	-0.55	-4.54	2.28x10 ⁻³
NT5DC4	71	-0.77	-4.55	2.28x10 ⁻³
ADAM19	4928	-0.48	-4.54	2.32x10 ⁻³
DGKD	4162	-0.38	-4.52	2.40x10 ⁻³
ABCA2	2913	-0.48	-4.50	2.56x10 ⁻³
HINT1	540	0.54	4.46	2.91x10 ⁻³
TRIM7	122	-0.64	-4.45	2.94x10 ⁻³
PIWIL4	117	0.63	4.45	2.96x10 ⁻³
ST14	819	-0.67	-4.44	2.96x10 ⁻³

IFI44L	357	0.90	4.43	3.00x10 ⁻³
C9orf123	134	0.56	4.38	3.66x10 ⁻³
CASC5	57	0.78	4.38	3.66x10 ⁻³
CYP1B1-AS1	76	-0.73	-4.36	3.93x10 ⁻³
AL137145.1	205	-0.70	-4.35	3.98x10 ⁻³
FUT4	360	0.45	4.35	3.98x10 ⁻³
MKNK1	4681	-0.44	-4.33	4.17x10 ⁻³
NUCB2	302	0.58	4.33	4.17x10 ⁻³
INHBA	20	0.88	4.32	4.30x10 ⁻³
AC061992.1	192	-0.63	-4.31	4.30x10 ⁻³
CCN JL	2099	-0.70	-4.30	4.30x10 ⁻³
GBP4	1456	0.80	4.30	4.30x10 ⁻³
MAD2L1	35	0.75	4.31	4.30x10 ⁻³
STAB1	3278	-0.61	-4.30	4.32x10 ⁻³
BMF	1012	-0.33	-4.27	4.65x10 ⁻³
MRPL32	137	0.50	4.27	4.65x10 ⁻³
PLK4	27	0.73	4.27	4.65x10 ⁻³
ACAT1	184	0.46	4.26	4.76x10 ⁻³
RP11-704M14.1	75	0.87	4.25	4.93x10 ⁻³
ACOT11	37	0.63	4.23	4.98x10 ⁻³
CLMN	1191	-0.44	-4.23	4.98x10 ⁻³
CMPK2	431	0.80	4.23	4.98x10 ⁻³
IFI44	544	0.84	4.24	4.98x10 ⁻³
SKA2	133	0.52	4.24	4.98x10 ⁻³
RFX2	2047	-0.61	-4.23	4.99x10 ⁻³
BATF2	224	0.81	4.20	5.27x10 ⁻³
RP11-443B7.1	198	-0.57	-4.21	5.27x10 ⁻³
RP11-473M20.7	5443	-0.55	-4.21	5.27x10 ⁻³
AL353791.1	104	-0.67	-4.19	5.40x10 ⁻³
FABP6	74	-0.80	-4.18	5.53x10 ⁻³
CES1	755	-0.71	-4.17	5.57x10 ⁻³
ETV7	89	0.86	4.18	5.57x10 ⁻³
MRPL13	60	0.55	4.18	5.57x10 ⁻³
NLRP12	4658	-0.46	-4.17	5.57x10 ⁻³
WDHD1	41	0.66	4.17	5.57x10 ⁻³
POLE2	25	0.71	4.14	6.04x10 ⁻³
COL17A1	101	0.85	4.13	6.17x10 ⁻³
KIAA1524	34	0.70	4.14	6.17x10 ⁻³
WDR76	98	0.60	4.11	6.65x10 ⁻³
RNASE4	146	-0.55	-4.11	6.72x10 ⁻³
SMTNL1	207	0.79	4.11	6.72x10 ⁻³
GBP5	3964	0.79	4.09	7.18x10 ⁻³
ATP8B4	407	0.57	4.08	7.27x10 ⁻³
CCDC64B	151	-0.81	-4.08	7.27x10 ⁻³
ELMO2	1763	-0.35	-4.07	7.46x10 ⁻³
SLFN13	409	0.49	4.06	7.71x10 ⁻³

ABCA13	197	0.83	4.05	8.00x10 ⁻³
SNRPG	103	0.65	4.05	8.00x10 ⁻³
CCT2	429	0.45	4.04	8.14x10 ⁻³
ATP2C2	77	0.78	4.02	8.46x10 ⁻³
SLC7A7	3945	-0.52	-4.03	8.46x10 ⁻³
TAF9	229	0.45	4.00	9.10x10 ⁻³
HMOX1	1708	-0.51	-4.00	9.24x10 ⁻³
FANCI	196	0.50	3.99	9.39x10 ⁻³
KIF15	24	0.76	3.99	9.39x10 ⁻³
RP11-1334A24.6	556	-0.52	-3.99	9.39x10 ⁻³
FAM53C	5007	-0.43	-3.98	9.66x10 ⁻³
RNASE3	701	0.81	3.97	9.66x10 ⁻³
VSIG4	299	-0.79	-3.97	9.66x10 ⁻³
GFI1	218	0.65	3.97	9.71x10 ⁻³
AREL1	2588	-0.33	-3.96	1.02x10 ⁻²
PI4K2B	275	0.54	3.95	1.02x10 ⁻²
KIF1B	2186	-0.43	-3.95	1.03x10 ⁻²
KIAA0101	37	0.81	3.94	1.06x10 ⁻²
HELLS	72	0.66	3.93	1.08x10 ⁻²
SIRPA	13345	-0.47	-3.93	1.09x10 ⁻²
CLC	1257	0.79	3.92	1.11x10 ⁻²
KDM4B	5004	-0.42	-3.92	1.11x10 ⁻²
THBS4	49	0.55	3.92	1.11x10 ⁻²
TNFSF14	1975	-0.38	-3.92	1.11x10 ⁻²
MAML3	738	-0.49	-3.91	1.13x10 ⁻²
GBP1	2308	0.76	3.90	1.16x10 ⁻²
ERG	63	0.80	3.89	1.19x10 ⁻²
FAM136A	221	0.30	3.88	1.19x10 ⁻²
RP11-701P16.2	113	-0.65	-3.89	1.19x10 ⁻²
SAMD4A	72	0.63	3.88	1.19x10 ⁻²
KB-1208A12.3	93	0.38	3.88	1.20x10 ⁻²
PFKFB3	6018	-0.58	-3.87	1.20x10 ⁻²
PRC1	90	0.62	3.88	1.20x10 ⁻²
CR1	6177	-0.52	-3.86	1.25x10 ⁻²
FBXO4	60	0.56	3.86	1.25x10 ⁻²
DLGAP5	28	0.79	3.86	1.26x10 ⁻²
EAF2	48	0.72	3.84	1.32x10 ⁻²
HDAC4	2592	-0.37	-3.84	1.32x10 ⁻²
NCAPG	41	0.75	3.84	1.32x10 ⁻²
PLXDC2	1377	-0.45	-3.84	1.32x10 ⁻²
SIRPB2	4171	-0.45	-3.84	1.32x10 ⁻²
EPSTI1	599	0.74	3.83	1.33x10 ⁻²
HPN	19	-0.74	-3.83	1.33x10 ⁻²
IL1R1	1115	-0.52	-3.83	1.33x10 ⁻²
LAMC1	134	-0.53	-3.83	1.33x10 ⁻²
TGFA	959	-0.51	-3.83	1.33x10 ⁻²

APLP2	13367	-0.41	-3.82	1.33×10^{-2}
CEP55	29	0.78	3.82	1.33×10^{-2}
PPARG	25	-0.73	-3.82	1.35×10^{-2}
CIT	46	0.75	3.81	1.35×10^{-2}
CTSG	1261	0.74	3.81	1.35×10^{-2}
ARHGAP19	870	-0.31	-3.81	1.38×10^{-2}
KIF13A	1756	-0.48	-3.80	1.38×10^{-2}
SSH2	13437	-0.44	-3.80	1.38×10^{-2}
PPT1	7521	-0.38	-3.80	1.38×10^{-2}
NSMCE2	92	0.52	3.79	1.41×10^{-2}
TLR5	1668	-0.50	-3.79	1.43×10^{-2}
CNTNAP3	1973	-0.66	-3.79	1.44×10^{-2}
AC108004.3	27	0.63	3.78	1.45×10^{-2}
CDCA7	59	0.61	3.78	1.45×10^{-2}
MMP14	124	-0.55	-3.77	1.45×10^{-2}
MRPL1	38	0.60	3.77	1.45×10^{-2}
AMPH	63	-0.74	-3.77	1.47×10^{-2}
MGAM	14190	-0.64	-3.77	1.47×10^{-2}
FAM219A	584	-0.30	-3.76	1.51×10^{-2}
IFIT1	1092	0.76	3.76	1.51×10^{-2}
NIF3L1	166	0.35	3.76	1.51×10^{-2}
SLC2A9	176	-0.40	-3.75	1.55×10^{-2}
HIP1	2520	-0.44	-3.74	1.60×10^{-2}
SLC2A5	220	0.75	3.74	1.60×10^{-2}
CENPE	33	0.74	3.73	1.61×10^{-2}
KDM6B	12490	-0.52	-3.73	1.62×10^{-2}
IL4R	10554	-0.49	-3.73	1.64×10^{-2}
ARHGEF11	3609	-0.42	-3.72	1.64×10^{-2}
CENPF	76	0.73	3.72	1.64×10^{-2}
AC004069.2	81	-0.61	-3.72	1.66×10^{-2}
LINC00482	120	-0.61	-3.72	1.66×10^{-2}
LRP1	3913	-0.55	-3.72	1.66×10^{-2}
AATK	4392	-0.47	-3.70	1.75×10^{-2}
ZFP36	10959	-0.41	-3.70	1.76×10^{-2}
DUSP1	9605	-0.62	-3.70	1.77×10^{-2}
NFIL3	2422	-0.47	-3.69	1.77×10^{-2}
RP11-20B24.7	183	-0.49	-3.69	1.79×10^{-2}
SH3PXD2B	114	-0.70	-3.69	1.79×10^{-2}
RP11-76E17.4	36	-0.74	-3.69	1.79×10^{-2}
DKFZP667F0711	113	-0.63	-3.68	1.81×10^{-2}
TNS3	591	-0.47	-3.68	1.84×10^{-2}
YEATS4	84	0.50	3.67	1.87×10^{-2}
PC	87	-0.51	-3.66	1.90×10^{-2}
MTMR3	7364	-0.38	-3.66	1.91×10^{-2}
MERTK	138	-0.59	-3.66	1.91×10^{-2}
AC091878.1	107	-0.56	-3.65	1.95×10^{-2}

RP11-1137G4.3	34	0.72	3.65	1.95x10 ⁻²
SVIP	235	0.59	3.65	1.95x10 ⁻²
KIF11	107	0.55	3.63	2.09x10 ⁻²
CHST15	9082	-0.46	-3.63	2.11x10 ⁻²
UGT2B11	22	0.75	3.62	2.11x10 ⁻²
NFKBIA	4244	-0.48	-3.62	2.12x10 ⁻²
DAB2	322	-0.47	-3.61	2.15x10 ⁻²
HRH2	2346	-0.53	-3.61	2.15x10 ⁻²
PPP1R3B	4579	-0.50	-3.62	2.15x10 ⁻²
RAB44	280	0.52	3.61	2.15x10 ⁻²
TECPR2	4937	-0.40	-3.61	2.15x10 ⁻²
ALOX15B	51	-0.75	-3.61	2.15x10 ⁻²
CXCR2	47021	-0.57	-3.61	2.15x10 ⁻²
GPER	153	-0.74	-3.61	2.18x10 ⁻²
AZU1	2651	0.72	3.60	2.20x10 ⁻²
PEX3	68	0.51	3.60	2.22x10 ⁻²
C2orf82	31	-0.60	-3.59	2.22x10 ⁻²
DCAF13	170	0.39	3.59	2.22x10 ⁻²
EMILIN2	3082	-0.44	-3.59	2.22x10 ⁻²
TBL1X	3560	-0.47	-3.59	2.22x10 ⁻²
TMEM150B	307	-0.51	-3.59	2.22x10 ⁻²
LSM5	77	0.48	3.58	2.26x10 ⁻²
TARM1	63	0.74	3.58	2.26x10 ⁻²
IL6R	14094	-0.41	-3.57	2.32x10 ⁻²
MARVELD1	480	-0.61	-3.57	2.32x10 ⁻²
PSMA4	642	0.51	3.57	2.32x10 ⁻²
RHAG	22	0.73	3.57	2.32x10 ⁻²
S1PR3	391	-0.54	-3.57	2.32x10 ⁻²
WDFY4	2382	-0.35	-3.57	2.32x10 ⁻²
WDR61	267	0.36	3.57	2.32x10 ⁻²
LAMP3	46	0.72	3.56	2.37x10 ⁻²
PROK2	9621	-0.54	-3.56	2.37x10 ⁻²
TIRAP	401	-0.28	-3.56	2.37x10 ⁻²
TPRKB	74	0.43	3.56	2.37x10 ⁻²
CDC45	36	0.73	3.55	2.38x10 ⁻²
CDH26	65	-0.51	-3.55	2.38x10 ⁻²
LINC00963	1937	-0.49	-3.55	2.38x10 ⁻²
SUCNR1	20	0.68	3.55	2.38x10 ⁻²
RP11-4F5.2	888	-0.40	-3.54	2.44x10 ⁻²
RP11-373D23.3	149	-0.56	-3.54	2.45x10 ⁻²
ISG15	1380	0.73	3.54	2.46x10 ⁻²
GAS7	7416	-0.52	-3.53	2.51x10 ⁻²
ATP6V1C2	30	0.60	3.53	2.51x10 ⁻²
RASSF2	23485	-0.39	-3.53	2.54x10 ⁻²
TCN1	688	0.73	3.53	2.54x10 ⁻²
ZCCHC24	200	-0.38	-3.52	2.60x10 ⁻²

DOCK2	7416	-0.31	-3.52	2.61x10 ⁻²
RP11-326C3.11	170	-0.42	-3.51	2.69x10 ⁻²
HES4	51	0.72	3.50	2.69x10 ⁻²
KIF14	19	0.65	3.50	2.72x10 ⁻²
CPAMD8	209	-0.46	-3.50	2.73x10 ⁻²
PLXND1	1991	-0.42	-3.50	2.73x10 ⁻²
VWA7	66	-0.53	-3.50	2.73x10 ⁻²
WIPF2	2153	-0.36	-3.49	2.76x10 ⁻²
CERS2	3222	-0.33	-3.49	2.77x10 ⁻²
HAUS1	77	0.54	3.49	2.77x10 ⁻²
TOP2A	111	0.71	3.49	2.77x10 ⁻²
MMP8	1533	0.71	3.49	2.77x10 ⁻²
ARHGEF40	5694	-0.54	-3.48	2.78x10 ⁻²
ITGAD	57	-0.62	-3.48	2.81x10 ⁻²
ADAMTS2	552	-0.70	-3.47	2.90x10 ⁻²
CENPH	38	0.62	3.47	2.90x10 ⁻²
PHF21A	5812	-0.37	-3.47	2.90x10 ⁻²
RP11-76E17.3	66	-0.67	-3.47	2.90x10 ⁻²
SUB1	677	0.52	3.46	2.91x10 ⁻²
HSPE1	98	0.52	3.46	2.94x10 ⁻²
PNPLA1	155	-0.50	-3.46	2.94x10 ⁻²
RP3-525N10.2	33	-0.68	-3.46	2.94x10 ⁻²
CD3D	476	0.53	3.43	3.14x10 ⁻²
CEPB	10987	-0.53	-3.44	3.14x10 ⁻²
FAM26F	213	0.57	3.43	3.14x10 ⁻²
FLT3	355	-0.69	-3.43	3.14x10 ⁻²
IQSEC1	8737	-0.36	-3.43	3.14x10 ⁻²
RNASEH2B	317	0.39	3.43	3.14x10 ⁻²
NIPSNAP3A	199	0.39	3.43	3.14x10 ⁻²
SLA	9171	-0.50	-3.43	3.14x10 ⁻²
HERC5	794	0.69	3.43	3.14x10 ⁻²
GCSAML	52	0.57	3.42	3.16x10 ⁻²
PRMT5	750	-0.44	-3.43	3.16x10 ⁻²
FBN2	197	-0.53	-3.42	3.16x10 ⁻²
OAS3	2041	0.68	3.42	3.16x10 ⁻²
PTX3	72	0.64	3.42	3.18x10 ⁻²
BAIAP2	369	-0.47	-3.42	3.19x10 ⁻²
ZWINT	55	0.67	3.42	3.19x10 ⁻²
BUB3	917	0.28	3.41	3.21x10 ⁻²
CYFIP1	1090	-0.37	-3.41	3.21x10 ⁻²
IL17RA	19125	-0.41	-3.41	3.21x10 ⁻²
IL18RAP	2094	-0.56	-3.41	3.21x10 ⁻²
NLRP3	1235	-0.48	-3.41	3.21x10 ⁻²
SRXN1	196	-0.49	-3.41	3.21x10 ⁻²
STIL	32	0.64	3.41	3.21x10 ⁻²
MPO	2413	0.69	3.41	3.22x10 ⁻²

VRK1	122	0.59	3.40	3.23x10 ⁻²
MRPL39	56	0.48	3.39	3.35x10 ⁻²
ABAT	965	-0.36	-3.39	3.35x10 ⁻²
CUX1	2758	-0.41	-3.39	3.35x10 ⁻²
MBP	9465	-0.42	-3.39	3.38x10 ⁻²
NDC80	55	0.57	3.39	3.38x10 ⁻²
RTDR1	47	-0.65	-3.39	3.38x10 ⁻²
ZSCAN18	211	-0.34	-3.39	3.38x10 ⁻²
SVIL	3671	-0.45	-3.38	3.39x10 ⁻²
ZNF503	42	-0.46	-3.38	3.39x10 ⁻²
ENY2	316	0.45	3.38	3.42x10 ⁻²
SLC8A1	955	-0.51	-3.38	3.42x10 ⁻²
UGGT1	1942	-0.29	-3.38	3.42x10 ⁻²
PRIM2	106	0.36	3.38	3.43x10 ⁻²
IL5RA	172	0.59	3.37	3.51x10 ⁻²
RP11-701P16.5	90	-0.57	-3.37	3.51x10 ⁻²
CASC3	5745	-0.40	-3.36	3.51x10 ⁻²
FOXM1	107	0.60	3.36	3.53x10 ⁻²
IFIT3	2993	0.67	3.36	3.53x10 ⁻²
RP11-802E16.3	317	-0.37	-3.36	3.53x10 ⁻²
C5AR1	19382	-0.45	-3.36	3.54x10 ⁻²
BICD2	3275	-0.36	-3.35	3.55x10 ⁻²
C1orf115	79	-0.45	-3.35	3.55x10 ⁻²
CEACAM6	578	0.69	3.35	3.55x10 ⁻²
CEACAM8	1080	0.68	3.36	3.55x10 ⁻²
ECHDC3	220	-0.65	-3.35	3.55x10 ⁻²
RP11-298I3.1	96	-0.56	-3.35	3.55x10 ⁻²
RPA3	93	0.49	3.35	3.60x10 ⁻²
FKBP3	181	0.38	3.34	3.60x10 ⁻²
MLF1IP	37	0.59	3.34	3.60x10 ⁻²
DEFA3	19589	0.64	3.34	3.60x10 ⁻²
DEFA4	2976	0.64	3.34	3.60x10 ⁻²
DYRK4	91	0.51	3.34	3.62x10 ⁻²
SORL1	39212	-0.46	-3.34	3.64x10 ⁻²
ALDH9A1	1170	-0.26	-3.33	3.66x10 ⁻²
BAIAP2-AS1	599	-0.42	-3.33	3.66x10 ⁻²
EPHB2	91	-0.50	-3.33	3.66x10 ⁻²
BPI	3539	0.67	3.33	3.72x10 ⁻²
COL8A2	89	-0.47	-3.33	3.73x10 ⁻²
RNASE1	114	-0.67	-3.33	3.73x10 ⁻²
TADA2B	1680	-0.31	-3.32	3.74x10 ⁻²
ARV1	73	0.36	3.32	3.75x10 ⁻²
NCOA6	1513	-0.30	-3.32	3.75x10 ⁻²
PSAT1	66	0.49	3.32	3.75x10 ⁻²
RNF175	461	-0.49	-3.32	3.75x10 ⁻²
CD1D	738	-0.39	-3.32	3.77x10 ⁻²

CDCA7L	287	0.49	3.32	3.77x10 ⁻²
RP11-67C2.2	330	-0.45	-3.32	3.78x10 ⁻²
C10orf105	295	-0.60	-3.31	3.79x10 ⁻²
ARHGAP26	7235	-0.43	-3.31	3.84x10 ⁻²
AQP9	27659	-0.41	-3.31	3.86x10 ⁻²
MDH1	490	0.44	3.30	3.89x10 ⁻²
SS18L2	107	0.44	3.30	3.89x10 ⁻²
NOTCH2	9263	-0.42	-3.30	3.90x10 ⁻²
CTC-246B18.8	69	-0.49	-3.30	3.94x10 ⁻²
RFC3	69	0.48	3.30	3.94x10 ⁻²
RP11-181G12.2	171	-0.36	-3.30	3.94x10 ⁻²
CDK1	28	0.68	3.29	3.96x10 ⁻²
TUFT1	132	-0.48	-3.29	3.96x10 ⁻²
C5orf56	725	0.41	3.29	4.00x10 ⁻²
ESPL1	61	0.63	3.29	4.00x10 ⁻²
IL10RB	3218	-0.30	-3.29	4.00x10 ⁻²
SLC11A1	22240	-0.50	-3.29	4.02x10 ⁻²
FBXO5	75	0.51	3.28	4.04x10 ⁻²
IFT57	120	0.48	3.28	4.04x10 ⁻²
KAT6A	3646	-0.43	-3.28	4.04x10 ⁻²
KDM5B	1009	-0.34	-3.28	4.04x10 ⁻²
KIAA0391	418	0.24	3.28	4.04x10 ⁻²
NOL3	87	-0.41	-3.28	4.04x10 ⁻²
SLC5A9	68	-0.63	-3.28	4.04x10 ⁻²
TCF19	193	0.49	3.28	4.04x10 ⁻²
DTL	44	0.67	3.27	4.04x10 ⁻²
MIS18A	38	0.50	3.27	4.04x10 ⁻²
ZNF608	207	-0.64	-3.27	4.04x10 ⁻²
DHFR	212	0.42	3.27	4.04x10 ⁻²
IRF2BPL	2936	-0.49	-3.27	4.05x10 ⁻²
STMN1	432	0.62	3.27	4.07x10 ⁻²
CYSLTR1	355	0.42	3.27	4.10x10 ⁻²
IL1B	1836	-0.45	-3.26	4.10x10 ⁻²
UQCRQ	182	0.50	3.26	4.12x10 ⁻²
CTNNA1	2898	-0.39	-3.25	4.16x10 ⁻²
DBN1	642	-0.51	-3.26	4.16x10 ⁻²
FAM49A	2729	-0.34	-3.26	4.16x10 ⁻²
RETN	980	0.67	3.26	4.16x10 ⁻²
UBE4B	1704	-0.33	-3.26	4.16x10 ⁻²
ZNF367	77	0.52	3.26	4.16x10 ⁻²
SLC29A3	186	-0.34	-3.25	4.17x10 ⁻²
CFLAR	14455	-0.35	-3.25	4.18x10 ⁻²
PTGFRN	47	-0.54	-3.25	4.19x10 ⁻²
ACADM	201	0.43	3.25	4.20x10 ⁻²
GBGT1	616	-0.43	-3.25	4.20x10 ⁻²
MATN2	27	0.54	3.25	4.20x10 ⁻²

MOCS2	93	0.35	3.25	4.20x10 ⁻²
SGOL2	40	0.60	3.24	4.20x10 ⁻²
FOSL2	7657	-0.36	-3.24	4.24x10 ⁻²
FANCL	75	0.52	3.24	4.25x10 ⁻²
GPR97	10028	-0.46	-3.24	4.28x10 ⁻²
PKNOX1	479	-0.26	-3.24	4.28x10 ⁻²
WASF2	8791	-0.36	-3.24	4.28x10 ⁻²
IGF1R	2866	-0.43	-3.23	4.28x10 ⁻²
LTF	14590	0.63	3.23	4.28x10 ⁻²
NCAPG2	149	0.48	3.23	4.28x10 ⁻²
ITGAM	12705	-0.44	-3.23	4.29x10 ⁻²
TIMM10	178	0.62	3.23	4.29x10 ⁻²
ADH5	436	0.36	3.23	4.30x10 ⁻²
RPSAP58	124	0.46	3.23	4.30x10 ⁻²
AC007278.3	212	-0.64	-3.22	4.35x10 ⁻²
ATP5C1	618	0.39	3.22	4.35x10 ⁻²
CRISPLD2	4330	-0.50	-3.22	4.35x10 ⁻²
ITSN1	199	-0.36	-3.22	4.35x10 ⁻²
RP13-580F15.2	68	0.55	3.22	4.35x10 ⁻²
COPS4	217	0.40	3.22	4.36x10 ⁻²
CCNA2	68	0.61	3.21	4.40x10 ⁻²
ZNF319	1121	-0.36	-3.21	4.43x10 ⁻²
CIDEB	67	-0.44	-3.21	4.43x10 ⁻²
MYLIP	1719	-0.36	-3.21	4.43x10 ⁻²
ATXN1	2498	-0.31	-3.21	4.44x10 ⁻²
DOK3	14016	-0.47	-3.21	4.44x10 ⁻²
SHROOM1	141	-0.52	-3.21	4.44x10 ⁻²
TBC1D30	82	-0.47	-3.20	4.45x10 ⁻²
TLE4	2706	-0.32	-3.20	4.45x10 ⁻²
ASPM	46	0.66	3.20	4.46x10 ⁻²
ZNF823	21	0.59	3.20	4.46x10 ⁻²
EEF1E1	26	0.54	3.20	4.47x10 ⁻²
RNF144A	391	0.46	3.20	4.47x10 ⁻²
SPC24	50	0.66	3.20	4.47x10 ⁻²
NCOR2	2947	-0.34	-3.20	4.48x10 ⁻²
SLC8A1-AS1	26	-0.54	-3.20	4.48x10 ⁻²
SNX27	3312	-0.33	-3.20	4.49x10 ⁻²
MLLT1	1133	-0.33	-3.19	4.50x10 ⁻²
MEGF6	891	-0.39	-3.19	4.50x10 ⁻²
ZNF746	3152	-0.43	-3.19	4.52x10 ⁻²
BEST1	1992	-0.38	-3.19	4.52x10 ⁻²
CBL	5966	-0.36	-3.19	4.52x10 ⁻²
GNS	6114	-0.37	-3.19	4.52x10 ⁻²
GPX7	90	0.42	3.19	4.52x10 ⁻²
MFN2	4153	-0.37	-3.19	4.52x10 ⁻²
RAD51	56	0.59	3.19	4.52x10 ⁻²

RP11-344B5.2	224	-0.46	-3.19	4.52x10 ⁻²
PYGL	15676	-0.47	-3.18	4.54x10 ⁻²
CHEK1	43	0.56	3.18	4.55x10 ⁻²
ZCCHC9	191	0.29	3.18	4.55x10 ⁻²
CPSF7	3652	-0.37	-3.18	4.56x10 ⁻²
ULK1	4884	-0.39	-3.18	4.57x10 ⁻²
AC096772.6	114	-0.34	-3.18	4.60x10 ⁻²
IFIT5	664	0.55	3.18	4.60x10 ⁻²
RPS27L	136	0.43	3.18	4.60x10 ⁻²
TYMS	163	0.64	3.18	4.60x10 ⁻²
LINC00211	173	-0.39	-3.17	4.62x10 ⁻²
NDEL1	3893	-0.37	-3.17	4.62x10 ⁻²
CLSPN	44	0.54	3.17	4.64x10 ⁻²
EZH2	173	0.46	3.17	4.64x10 ⁻²
FAM71F2	105	-0.48	-3.17	4.64x10 ⁻²
LPCAT3	1538	-0.37	-3.17	4.64x10 ⁻²
TG	105	-0.52	-3.17	4.64x10 ⁻²
EXOSC9	265	0.35	3.16	4.69x10 ⁻²
PSMD10	202	0.36	3.16	4.70x10 ⁻²
TOMM5	44	0.41	3.16	4.72x10 ⁻²
LINC00593	37	-0.54	-3.16	4.74x10 ⁻²
CXCR1	32208	-0.47	-3.16	4.78x10 ⁻²
ITPRIP	3718	-0.38	-3.15	4.80x10 ⁻²
NDUFA4	329	0.53	3.15	4.80x10 ⁻²
PWP1	314	0.26	3.15	4.80x10 ⁻²
ZNF480	105	0.38	3.15	4.80x10 ⁻²
HMGN1	1203	0.35	3.15	4.80x10 ⁻²
MSN	34989	-0.39	-3.15	4.80x10 ⁻²
NSMCE4A	260	0.31	3.15	4.80x10 ⁻²
SEMA6A	35	0.48	3.15	4.80x10 ⁻²
SSB	304	0.39	3.15	4.80x10 ⁻²
TRIAP1	87	0.38	3.15	4.83x10 ⁻²
PADI2	8617	-0.45	-3.15	4.84x10 ⁻²
SLC2A3	16672	-0.43	-3.14	4.88x10 ⁻²
HAUS2	224	0.28	3.14	4.89x10 ⁻²
PSMG1	77	0.44	3.14	4.90x10 ⁻²
DZIP1L	33	0.63	3.14	4.95x10 ⁻²
ARNTL2	30	0.51	3.13	4.96x10 ⁻²
TIPIN	35	0.47	3.13	4.97x10 ⁻²
LDLRAD3	118	-0.48	-3.13	4.97x10 ⁻²
NRG1	159	-0.43	-3.13	4.97x10 ⁻²
ASPH	963	-0.51	-3.13	4.98x10 ⁻²

Log2FC indicates Log2 fold change; Stat indicates the results from Wald statistic; and B-H indicates P-value after Benjamini-Hochberg correction for false discovery rate.

Table II. The 164 differentially expressed genes between controls and aneurysmal SAH (aSAH) patients before and after RIC treatment.

DESeq2	aSAH untreated vs. treated					untreated controls vs. untreated aSAH					untreated controls vs. treated aSAH				
	GENE	Mean	Log2FC	SE	Stat	P-value	Mean	Log2FC	SE	Stat	P-value	Mean	Log2FC	SE	Stat
HTRA1	98	-1.28	0.19	-6.73	2.47x10 ⁻⁷	86	2.25	0.27	8.26	5.00x10 ^{-13*}	39	0.63	0.27	2.32	8.09x10 ⁻²
MYO7A	177	-1.00	0.17	-5.80	1.61x10 ⁻⁵	173	1.59	0.20	7.88	9.69x10 ^{-12*}	109	0.34	0.18	1.89	1.69x10 ⁻¹
OLR1	136	1.19	0.20	5.82	1.61x10 ⁻⁵	40	0.83	0.34	2.49	3.59x10 ⁻²	118	2.44	0.31	7.89	4.65x10 ^{-12*}
CRISP3	394	1.13	0.20	5.66	2.93x10 ⁻⁵	153	0.46	0.33	1.39	2.72x10 ⁻¹	369	1.85	0.32	5.80	7.91x10 ^{-7*}
SERPINB10	108	1.01	0.20	5.13	3.24x10 ⁻⁴	38	0.89	0.30	3.00	1.01x10 ⁻²	94	2.23	0.30	7.34	1.26x10 ^{-10*}
STAT5B	13869	-0.43	0.08	-5.04	4.74x10 ⁻⁴	14359	0.76	0.15	5.27	4.52x10 ^{-6*}	12921	0.34	0.14	2.33	8.02x10 ⁻²
BCL2L15	74	0.93	0.19	4.95	6.44x10 ⁻⁴	45	0.03	0.20	0.16	9.16x10 ⁻¹	80	1.41	0.24	5.85	6.46x10 ^{-7*}
SSH1	2477	-0.49	0.10	-4.92	7.15x10 ⁻⁴	2519	0.86	0.15	5.86	3.48x10 ^{-7*}	2221	0.38	0.15	2.46	6.14x10 ⁻²
DNAH17	1640	-0.56	0.11	-4.85	8.96x10 ⁻⁴	1412	1.45	0.22	6.56	1.27x10 ^{-8*}	1121	0.84	0.21	4.02	1.21x10 ⁻³
ANLN	39	0.91	0.19	4.85	8.96x10 ⁻⁴	21	0.64	0.23	2.73	2.00x10 ⁻²	37	1.79	0.22	8.22	5.85x10 ^{-13*}
RP11-473M20.5	362	-0.79	0.16	-4.81	9.70x10 ⁻⁴	394	0.99	0.20	4.95	1.56x10 ^{-5*}	298	0.07	0.20	0.35	8.43x10 ⁻¹
HAUS4	1226	-0.57	0.12	-4.80	9.70x10 ⁻⁴	1319	0.80	0.18	4.49	9.42x10 ^{-5*}	1119	0.19	0.17	1.12	4.59x10 ⁻¹
MANSC1	2500	-0.68	0.14	-4.78	1.03x10 ⁻³	2417	1.14	0.18	6.23	7.17x10 ^{-8*}	1959	0.47	0.20	2.32	8.12x10 ⁻²
MS4A3	355	0.97	0.20	4.76	1.12x10 ⁻³	166	0.13	0.28	0.46	7.47x10 ⁻¹	362	1.70	0.28	6.02	2.63x10 ^{-7*}
RP5-968J1.1	49	-0.73	0.15	-4.75	1.15x10 ⁻³	49	1.15	0.21	5.51	1.72x10 ^{-6*}	37	0.33	0.21	1.61	2.53x10 ⁻¹
ETS2	2895	-0.65	0.14	-4.72	1.20x10 ⁻³	2937	1.07	0.18	5.86	3.48x10 ^{-7*}	2334	0.32	0.17	1.91	1.65x10 ⁻¹
RP11-1D12.2	26	0.93	0.20	4.57	2.19x10 ⁻³	7	0.54	0.35	1.54	2.19x10 ⁻¹	23	2.24	0.32	6.93	1.45x10 ^{-9*}
DGKD	4162	-0.38	0.08	-4.52	2.40x10 ⁻³	4483	0.62	0.10	6.34	4.20x10 ^{-8*}	4143	0.25	0.11	2.34	7.78x10 ⁻²
TRIM7	122	-0.64	0.14	-4.45	2.94x10 ⁻³	126	0.92	0.15	6.32	4.48x10 ^{-8*}	105	0.28	0.17	1.62	2.52x10 ⁻¹
ST14	819	-0.67	0.15	-4.44	2.96x10 ⁻³	886	0.88	0.17	5.06	1.03x10 ^{-5*}	719	0.14	0.18	0.78	6.26x10 ⁻¹
PIWIL4	117	0.63	0.14	4.45	2.96x10 ⁻³	86	0.42	0.13	3.31	4.26x10 ⁻³	118	1.21	0.16	7.36	1.06x10 ^{-10*}
CASC5	57	0.78	0.18	4.38	3.66x10 ⁻³	40	0.29	0.20	1.45	2.47x10 ⁻¹	59	1.27	0.19	6.87	2.14x10 ^{-9*}
CYP1B1-AS1	76	-0.73	0.17	-4.36	3.93x10 ⁻³	75	1.23	0.25	5.01	1.27x10 ^{-5*}	54	0.34	0.23	1.47	3.05x10 ⁻¹
AL137145.1	205	-0.70	0.16	-4.35	3.98x10 ⁻³	208	1.12	0.19	5.82	4.24x10 ^{-7*}	160	0.30	0.19	1.57	2.68x10 ⁻¹
FUT4	360	0.45	0.10	4.35	3.98x10 ⁻³	328	0.25	0.07	3.57	1.98x10 ⁻³	397	0.75	0.09	8.22	5.85x10 ^{-13*}
MKNK1	4681	-0.44	0.10	-4.33	4.17x10 ⁻³	4460	1.01	0.19	5.20	5.95x10 ^{-6*}	3895	0.54	0.19	2.91	2.42x10 ⁻²
INHBA	20	0.88	0.20	4.32	4.30x10 ⁻³	8	0.75	0.35	2.14	7.43x10 ⁻²	17	1.84	0.32	5.70	1.28x10 ^{-6*}
AC061992.1	192	-0.63	0.15	-4.31	4.30x10 ⁻³	158	1.75	0.24	7.30	2.81x10 ^{-10*}	114	1.01	0.22	4.55	1.97x10 ⁻⁴
GBP4	1456	0.80	0.19	4.30	4.30x10 ⁻³	1927	-1.07	0.20	-5.36	3.14x10 ^{-6*}	2517	0.07	0.22	0.34	8.51x10 ⁻¹
STAB1	3278	-0.61	0.14	-4.30	4.32x10 ⁻³	3351	1.04	0.14	7.20	5.63x10 ^{-10*}	2712	0.32	0.13	2.50	5.70x10 ⁻²
BMF	1012	-0.33	0.08	-4.27	4.65x10 ⁻³	1148	0.46	0.08	5.83	4.03x10 ^{-7*}	1081	0.13	0.09	1.52	2.88x10 ⁻¹
CLMN	1191	-0.44	0.10	-4.23	4.98x10 ⁻³	1292	0.68	0.13	5.41	2.60x10 ^{-6*}	1155	0.21	0.12	1.75	2.09x10 ⁻¹
IFI44	544	0.84	0.20	4.24	4.98x10 ⁻³	698	-1.45	0.32	-4.49	9.23x10 ^{-5*}	804	-0.73	0.30	-2.42	6.70x10 ⁻²
RFX2	2047	-0.61	0.14	-4.23	4.99x10 ⁻³	1849	1.30	0.22	6.00	1.91x10 ^{-7*}	1489	0.67	0.22	3.04	1.80x10 ⁻²

RP11-473M20.7	5443	-0.55	0.13	-4.21	5.27x10 ⁻³	5398	0.97	0.18	5.34	3.35x10 ^{-6*}	4601	0.41	0.19	2.16	1.08x10 ⁻¹	
NLRP12	4658	-0.46	0.11	-4.17	5.57x10 ⁻³	4797	0.78	0.16	4.86	2.29x10 ^{-5*}	4292	0.34	0.17	1.98	1.47x10 ⁻¹	
COL17A1	101	0.85	0.21	4.13	6.17x10 ⁻³	30	0.91	0.26	3.48	2.63x10 ⁻³	89	2.46	0.30	8.14	8.38x10 ^{-13*}	
RNASE4	146	-0.55	0.13	-4.11	6.72x10 ⁻³	146	1.00	0.19	5.33	3.57x10 ^{-6*}	121	0.39	0.18	2.23	9.61x10 ⁻²	
GBP5	3964	0.79	0.19	4.09	7.18x10 ⁻³	4980	-1.09	0.23	-4.77	3.13x10 ^{-5*}	6743	0.16	0.26	0.63	7.02x10 ⁻¹	
ATP8B4	407	0.57	0.14	4.08	7.27x10 ⁻³	360	0.17	0.14	1.19	3.57x10 ⁻¹	455	0.81	0.14	5.84	6.47x10 ^{-7*}	
ABCA13	197	0.83	0.21	4.05	8.00x10 ⁻³	78	0.81	0.34	2.38	4.53x10 ⁻²	171	1.96	0.32	6.16	1.22x10 ^{-7*}	
SLC7A7	3945	-0.52	0.13	-4.03	8.46x10 ⁻³	4283	0.77	0.13	5.87	3.43x10 ^{-7*}	3684	0.18	0.12	1.47	3.05x10 ⁻¹	
RP11-1334A24.6	556	-0.52	0.13	-3.99	9.39x10 ⁻³	577	0.81	0.18	4.55	7.27x10 ^{-5*}	505	0.30	0.19	1.61	2.56x10 ⁻¹	
KIF15	24	0.76	0.19	3.99	9.39x10 ⁻³	17	0.13	0.24	0.57	6.81x10 ⁻¹	26	1.19	0.24	4.98	3.62x10 ^{-5*}	
VSIG4	299	-0.79	0.20	-3.97	9.66x10 ⁻³	240	1.94	0.29	6.78	4.08x10 ^{-9*}	109	0.20	0.23	0.87	5.80x10 ⁻¹	
RNASE3	701	0.81	0.20	3.97	9.66x10 ⁻³	88	0.64	0.33	1.97	1.04x10 ⁻¹	163	1.60	0.32	5.03	3.01x10 ^{-5*}	
KIAA0101	37	0.81	0.21	3.94	1.06x10 ⁻³	15	0.52	0.25	2.04	9.14x10 ⁻²	35	1.97	0.28	7.06	6.74x10 ^{-10*}	
SIRPA	13345	-0.47	0.12	-3.93	1.09x10 ⁻³	13087	0.94	0.18	5.30	3.99x10 ^{-6*}	11456	0.46	0.18	2.56	5.05x10 ⁻²	
ERG	63	0.80	0.21	3.89	1.19x10 ⁻²	24	0.83	0.27	3.09	7.94x10 ⁻³	55	2.20	0.28	7.88	4.65x10 ^{-12*}	
PFKFB3	6018	-0.58	0.15	-3.87	1.20x10 ⁻²	4986	1.55	0.26	5.87	3.33x10 ^{-7*}	3844	0.91	0.26	3.55	4.91x10 ⁻³	
PRC1	90	0.62	0.16	3.88	1.20x10 ⁻²	80	-0.01	0.12	-0.11	9.41x10 ⁻¹	105	0.79	0.16	4.99	3.36x10 ^{-5*}	
FBXO4	60	0.56	0.14	3.86	1.25x10 ⁻²	81	-0.65	0.14	-4.52	8.22x10 ^{-5*}	96	-0.04	0.13	-0.31	8.65x10 ⁻¹	
DLGAP5	28	0.79	0.20	3.86	1.26x10 ⁻²	15	0.56	0.27	2.08	8.39x10 ⁻²	27	1.79	0.23	7.83	6.29x10 ^{-12*}	
HDAC4	2592	-0.37	0.10	-3.84	1.32x10 ⁻²	2644	0.81	0.16	5.02	1.21x10 ^{-5*}	2366	0.38	0.14	2.73	3.59x10 ⁻²	
NCAPG	41	0.75	0.20	3.84	1.32x10 ⁻²	26	0.41	0.23	1.81	1.41x10 ⁻¹	41	1.43	0.21	6.75	4.43x10 ^{-9*}	
HPN	19	-0.74	0.19	-3.83	1.33x10 ⁻²	17	1.68	0.25	6.64	8.73x10 ^{-9*}	11	0.71	0.26	2.74	3.46x10 ⁻²	
IL1R1	1115	-0.52	0.14	-3.83	1.33x10 ⁻²	1038	1.13	0.21	5.27	4.47x10 ^{-6*}	869	0.58	0.21	2.73	3.59x10 ⁻²	
LAMC1	134	-0.53	0.14	-3.83	1.33x10 ⁻²	144	0.76	0.15	5.18	6.56x10 ^{-6*}	126	0.21	0.16	1.28	3.85x10 ⁻¹	
CEP55	29	0.78	0.20	3.82	1.33x10 ⁻²	16	0.41	0.25	1.63	1.88x10 ⁻¹	29	1.59	0.24	6.72	5.24x10 ^{-9*}	
PPARG	25	-0.73	0.19	-3.82	1.35x10 ⁻²	19	2.13	0.27	7.85	9.69x10 ^{-12*}	12	1.20	0.28	4.36	3.92x10 ⁻⁴	
CTSG	1261	0.74	0.19	3.81	1.35x10 ⁻²	74	1.02	0.34	3.01	9.92x10 ⁻³	162	2.03	0.33	6.21	9.61x10 ^{-8*}	
CIT	46	0.75	0.20	3.81	1.35x10 ⁻²	35	-0.01	0.20	-0.05	9.76x10 ⁻¹	52	1.07	0.19	5.74	1.03x10 ^{-6*}	
TLR5	1668	-0.50	0.13	-3.79	1.43x10 ⁻²	1515	1.16	0.23	5.16	7.00x10 ^{-6*}	1281	0.65	0.22	2.90	2.42x10 ⁻²	
CNTNAP3	1973	-0.66	0.17	-3.79	1.44x10 ⁻²	1586	1.48	0.30	5.00	1.30x10 ^{-5*}	1265	0.90	0.30	2.98	2.04x10 ⁻²	
MMP14	124	-0.55	0.14	-3.77	1.45x10 ⁻²	115	1.25	0.18	6.91	2.16x10 ^{-9*}	93	0.62	0.17	3.74	2.82x10 ⁻³	
AMPH	63	-0.74	0.20	-3.77	1.47x10 ⁻²	53	1.99	0.27	7.46	1.16x10 ^{-10*}	31	0.91	0.25	3.68	3.35x10 ⁻³	
FAM219A	584	-0.30	0.08	-3.76	1.51x10 ⁻²	647	0.49	0.09	5.35	3.24x10 ^{-6*}	612	0.19	0.09	2.18	1.04x10 ⁻¹	
SLC2A5	220	0.75	0.20	3.74	1.60x10 ⁻²	97	0.54	0.22	2.42	4.19x10 ⁻²	208	1.94	0.27	7.18	3.16x10 ^{-10*}	
IL4R	10554	-0.49	0.13	-3.73	1.64x10 ⁻²	9961	1.10	0.19	5.74	6.00x10 ^{-7*}	8434	0.57	0.19	3.03	1.85x10 ⁻²	
CENPF	76	0.73	0.20	3.72	1.64x10 ⁻²	57	0.06	0.20	0.31	8.30x10 ⁻¹	85	1.10	0.19	5.87	5.89x10 ^{-7*}	
LINC00482	120	-0.61	0.16	-3.72	1.66x10 ⁻²	108	1.35	0.22	6.11	1.17x10 ^{-7*}	85	0.67	0.22	2.99	2.01x10 ⁻²	
AATK	4392	-0.47	0.13	-3.70	1.75x10 ⁻²	4274	0.94	0.15	6.19	8.69x10 ^{-8*}	3805	0.50	0.17	2.87	2.62x10 ⁻²	
ZFP36	10959	-0.41	0.11	-3.70	1.76x10 ⁻²	11298	0.77	0.15	5.13	8.11x10 ^{-6*}	10170	0.35	0.15	2.35	7.61x10 ⁻²	

DUSP1	9605	-0.62	0.17	-3.70	1.77x10 ⁻²	9807	1.02	0.19	5.49	1.83x10 ^{-6*}	7874	0.30	0.19	1.56	2.71x10 ⁻¹
NFIL3	2422	-0.47	0.13	-3.69	1.77x10 ⁻²	2530	0.77	0.17	4.68	4.59x10 ^{-5*}	2240	0.30	0.17	1.71	2.21x10 ⁻¹
RP11-20B24.7	183	-0.49	0.13	-3.69	1.79x10 ⁻²	168	1.16	0.18	6.40	2.91x10 ^{-8*}	144	0.65	0.19	3.45	6.37x10 ⁻³
SH3PXD2B	114	-0.70	0.19	-3.69	1.79x10 ⁻²	101	1.75	0.29	5.95	2.39x10 ^{-7*}	61	0.70	0.26	2.69	3.87x10 ⁻²
DKFZP667F0711	113	-0.63	0.17	-3.68	1.81x10 ⁻²	114	1.09	0.23	4.77	3.13x10 ^{-5*}	88	0.33	0.22	1.48	3.03x10 ⁻¹
MTMR3	7364	-0.38	0.10	-3.66	1.91x10 ⁻²	7804	0.67	0.14	4.74	3.61x10 ^{-5*}	7138	0.28	0.14	1.97	1.49x10 ⁻¹
MERTK	138	-0.59	0.16	-3.66	1.91x10 ⁻²	141	1.00	0.21	4.63	5.47x10 ^{-5*}	113	0.30	0.21	1.44	3.18x10 ⁻¹
AC091878.1	107	-0.56	0.15	-3.65	1.95x10 ⁻²	86	1.58	0.28	5.71	6.72x10 ^{-7*}	67	0.98	0.27	3.61	4.10x10 ⁻³
KIF11	107	0.55	0.15	3.63	2.09x10 ⁻²	86	0.35	0.15	2.28	5.69x10 ⁻²	112	1.01	0.16	6.16	1.24x10 ^{-7*}
NFKBIA	4244	-0.48	0.13	-3.62	2.12x10 ⁻²	4186	0.97	0.14	7.12	7.27x10 ^{-10*}	3635	0.46	0.14	3.24	1.11x10 ⁻²
TECPR2	4937	-0.40	0.11	-3.61	2.15x10 ⁻²	4872	0.85	0.17	5.10	8.89x10 ^{-6*}	4416	0.46	0.17	2.69	3.91x10 ⁻²
GPER	153	-0.74	0.20	-3.61	2.18x10 ⁻²	128	1.99	0.29	6.93	1.96x10 ^{-9*}	74	0.86	0.28	3.06	1.71x10 ⁻²
AZU1	2651	0.72	0.20	3.60	2.20x10 ⁻²	183	0.96	0.33	2.96	1.11x10 ⁻²	322	1.72	0.32	5.36	6.56x10 ^{-6*}
PEX3	68	0.51	0.14	3.60	2.22x10 ⁻²	102	-0.82	0.13	-6.11	1.18x10 ^{-7*}	117	-0.26	0.13	-1.94	1.55x10 ⁻¹
TMEM150B	307	-0.51	0.14	-3.59	2.22x10 ⁻²	294	1.07	0.15	7.01	1.26x10 ^{-9*}	251	0.53	0.17	3.20	1.20x10 ⁻²
TARM1	63	0.74	0.21	3.58	2.26x10 ⁻²	14	1.16	0.30	3.86	8.05x10 ⁻⁴	26	2.00	0.30	6.67	6.89x10 ^{-9*}
MARVELD1	480	-0.61	0.17	-3.57	2.32x10 ⁻²	473	1.11	0.16	6.82	3.59x10 ^{-9*}	382	0.41	0.18	2.30	8.40x10 ⁻²
S1PR3	391	-0.54	0.15	-3.57	2.32x10 ⁻²	436	0.66	0.14	4.72	3.80x10 ^{-5*}	382	0.11	0.17	0.67	6.80x10 ⁻¹
RHAG	22	0.73	0.21	3.57	2.32x10 ⁻²	12	0.73	0.33	2.21	6.52x10 ⁻²	20	1.70	0.28	5.99	3.04x10 ^{-7*}
LAMP3	46	0.72	0.20	3.56	2.37x10 ⁻²	68	-1.56	0.28	-5.51	1.67x10 ^{-6*}	79	-0.66	0.28	-2.34	7.82x10 ⁻²
PROK2	9621	-0.54	0.15	-3.56	2.37x10 ⁻²	8807	1.20	0.25	4.71	3.99x10 ^{-5*}	7119	0.60	0.25	2.45	6.30x10 ⁻²
LINC00963	1937	-0.49	0.14	-3.55	2.38x10 ⁻²	1822	1.13	0.17	6.79	3.97x10 ^{-9*}	1544	0.59	0.16	3.57	4.58x10 ⁻³
CDC45	36	0.73	0.21	3.55	2.38x10 ⁻²	13	0.70	0.26	2.65	2.42x10 ⁻²	33	2.14	0.29	7.46	6.10x10 ^{-11*}
SUCNR1	20	0.68	0.19	3.55	2.38x10 ⁻²	12	0.53	0.23	2.27	5.71x10 ⁻²	19	1.50	0.24	6.28	6.80x10 ^{-8*}
RP11-373D23.3	149	-0.56	0.16	-3.54	2.45x10 ⁻²	137	1.32	0.24	5.43	2.37x10 ^{-6*}	105	0.60	0.22	2.76	3.32x10 ⁻²
GAS7	7416	-0.52	0.15	-3.53	2.51x10 ⁻²	6704	1.27	0.18	7.19	5.63x10 ^{-10*}	5545	0.70	0.18	3.96	1.48x10 ⁻³
RASSF2	23485	-0.39	0.11	-3.53	2.54x10 ⁻²	25670	0.59	0.13	4.55	7.41x10 ^{-5*}	23572	0.20	0.13	1.50	2.93x10 ⁻¹
TCN1	688	0.73	0.21	3.53	2.54x10 ⁻²	232	0.55	0.24	2.27	5.72x10 ⁻²	372	1.49	0.26	5.77	9.20x10 ^{-7*}
ZCCHC24	200	-0.38	0.11	-3.52	2.60x10 ⁻²	204	0.77	0.13	5.83	4.13x10 ^{-7*}	187	0.40	0.14	2.82	2.96x10 ⁻²
KIF14	19	0.65	0.19	3.50	2.72x10 ⁻²	12	0.64	0.27	2.37	4.61x10 ⁻²	17	1.45	0.24	5.93	4.12x10 ^{-7*}
TOP2A	111	0.71	0.20	3.49	2.77x10 ⁻²	72	0.38	0.25	1.50	2.31x10 ⁻¹	111	1.42	0.20	7.21	2.86x10 ^{-10*}
MMP8	1533	0.71	0.20	3.49	2.77x10 ⁻²	425	1.05	0.36	2.93	1.20x10 ⁻²	1275	2.31	0.34	6.84	2.47x10 ^{-9*}
ARHGEF40	5694	-0.54	0.16	-3.48	2.78x10 ⁻²	5390	1.09	0.20	5.35	3.33x10 ^{-6*}	4535	0.53	0.21	2.50	5.74x10 ⁻²
ADAMTS2	552	-0.70	0.20	-3.47	2.90x10 ⁻²	379	2.49	0.38	6.57	1.25x10 ^{-8*}	95	1.03	0.35	2.96	2.16x10 ⁻²
PHF21A	5812	-0.37	0.11	-3.47	2.90x10 ⁻²	5832	0.81	0.17	4.77	3.21x10 ^{-5*}	5288	0.42	0.17	2.53	5.41x10 ⁻²
PNPLA1	155	-0.50	0.15	-3.46	2.94x10 ⁻²	160	0.86	0.16	5.31	3.83x10 ^{-6*}	138	0.33	0.17	1.89	1.70x10 ⁻¹
CEBPB	10987	-0.53	0.16	-3.44	3.14x10 ⁻²	10791	1.04	0.18	5.67	7.96x10 ^{-7*}	9016	0.44	0.19	2.37	7.38x10 ⁻²
FLT3	355	-0.69	0.20	-3.43	3.14x10 ⁻²	323	1.51	0.28	5.40	2.65x10 ^{-6*}	216	0.54	0.28	1.94	1.57x10 ⁻¹
HERC5	794	0.69	0.20	3.43	3.14x10 ⁻²	1023	-1.33	0.29	-4.62	5.69x10 ^{-5*}	1205	-0.51	0.29	-1.79	1.97x10 ⁻¹

RAD51	56	0.59	0.18	3.19	4.52x10 ⁻²	41	0.23	0.15	1.54	2.16x10 ⁻¹	60	1.15	0.20	5.75	1.01x10 ⁻⁶ *	
PYGL	15676	-0.47	0.15	-3.18	4.54x10 ⁻²	14316	1.11	0.21	5.33	3.50x10 ⁻⁶ *	12455	0.65	0.22	2.97	2.10x10 ⁻²	
CHEK1	43	0.56	0.18	3.18	4.55x10 ⁻²	36	0.10	0.14	0.68	6.21x10 ⁻¹	48	0.90	0.18	4.96	3.96x10 ⁻⁵ *	
TYMS	163	0.64	0.20	3.18	4.60x10 ⁻²	90	0.67	0.22	3.04	9.14x10 ⁻³	151	1.71	0.23	7.45	6.25x10 ⁻¹¹ *	
TG	105	-0.52	0.16	-3.17	4.64x10 ⁻²	93	1.32	0.19	6.97	1.64x10 ⁻⁹ *	76	0.73	0.20	3.69	3.29x10 ⁻³	
CLSPN	44	0.54	0.17	3.17	4.64x10 ⁻²	34	0.46	0.18	2.61	2.72x10 ⁻²	45	1.14	0.19	6.15	1.26x10 ⁻⁷ *	
ZNF480	105	0.38	0.12	3.15	4.80x10 ⁻²	153	-0.63	0.13	-4.95	1.58x10 ⁻⁵ *	171	-0.22	0.12	-1.80	1.94x10 ¹	
NSMCE4A	260	0.31	0.10	3.15	4.80x10 ⁻²	386	-0.62	0.12	-5.10	8.94x10 ⁻⁶ *	425	-0.29	0.12	-2.38	7.18x10 ⁻²	
SSB	304	0.39	0.12	3.15	4.80x10 ⁻²	428	-0.60	0.13	-4.62	5.67x10 ⁻⁵ *	484	-0.16	0.13	-1.19	4.21x10 ⁻¹	
SLC2A3	16672	-0.43	0.14	-3.14	4.88x10 ⁻²	15577	1.00	0.21	4.84	2.40x10 ⁻⁵ *	13863	0.59	0.22	2.73	3.53x10 ⁻²	
DZIP1L	33	0.63	0.20	3.14	4.95x10 ⁻²	15	0.94	0.23	4.13	3.31x10 ⁻⁴	29	1.96	0.27	7.39	8.91x10 ⁻¹¹ *	
ARNTL2	30	0.51	0.16	3.13	4.96x10 ⁻²	25	0.33	0.18	1.77	1.49x10 ⁻¹	32	0.93	0.17	5.46	4.11x10 ⁻⁶ *	
ASPH	963	-0.51	0.16	-3.13	4.98x10 ⁻²	923	1.09	0.20	5.44	2.28x10 ⁻⁶ *	768	0.50	0.20	2.49	5.78x10 ⁻²	

Log2FC indicates Log2 fold change; SE indicates standard error; Stat indicates the results from Wald statistic; and * indicates Bonferroni corrected significant P<1.1X10⁻⁴ (P<0.05/451 DE genes).

Table III. Overlap between the differentially expressed genes and differentially methylated CpG sites.

Chr	Gene start position	Gene end position	Gene	CpG site position	CpG site p-value
1	9101426	9129887	SLC2A5	9100067	3.29x10 ⁻³
1	9101426	9129887	SLC2A5	9147808	9.31x10 ⁻³
1	9101426	9129887	SLC2A5	9243783	8.36x10 ⁻⁴
1	9101426	9129887	SLC2A5	9368498	6.38x10 ⁻³
1	36197712	36235551	CLSPN	36029011	2.27x10 ⁻³
1	47023078	47069966	MKNK1	46956771	7.41x10 ⁻³
1	200520624	200589862	KIF14	200512245	5.72x10 ⁻³
1	212208894	212278348	DTL	212266836	3.94x10 ⁻³
1	214776531	214837914	CENPF	214846563	4.10x10 ⁻³
1	223282747	223316624	TLR5	223487288	5.21x10 ⁻³
2	7057522	7184309	RNF144A	6922444	8.81x10 ⁻³
2	7057522	7184309	RNF144A	7148323	1.56x10 ⁻⁴
2	7057522	7184309	RNF144A	7148362	5.43x10 ⁻³
2	7057522	7184309	RNF144A	7213398	2.32x10 ⁻³
2	102759235	102796334	IL1R1	102647671	2.18x10 ⁻³
2	102759235	102796334	IL1R1	102647718	9.45x10 ⁻³
2	128848753	128953249	UGGT1	128973012	7.59x10 ⁻³
2	128848753	128953249	UGGT1	129033961	2.77x10 ⁻³
2	128848753	128953249	UGGT1	129037628	7.08x10 ⁻³
2	234296799	234380743	DGKD	234093536	5.06x10 ⁻³
2	234296799	234380743	DGKD	234394437	6.31x10 ⁻³
2	239969863	240322643	HDAC4	239756133	7.05x10 ⁻³
2	239969863	240322643	HDAC4	239763625	9.61x10 ⁻³
2	239969863	240322643	HDAC4	240199099	9.29x10 ⁻³
2	239969863	240322643	HDAC4	240302529	2.14x10 ⁻³
3	12329348	12475855	PPARG	12110937	7.86x10 ⁻³
3	12329348	12475855	PPARG	12482963	1.52x10 ⁻³
3	44803208	44894748	KIF15	44902961	6.07x10 ⁻³
3	44803208	44894748	KIF15	45106462	5.07x10 ⁻³
3	46477495	46505161	LTF	46750030	9.61x10 ⁻³
3	52529355	52558511	STAB1	52389151	7.61x10 ⁻⁴
3	52529355	52558511	STAB1	52566526	7.08x10 ⁻³
3	71820805	71834357	PROK2	71721378	2.46x10 ⁻³
3	71820805	71834357	PROK2	71932814	8.91x10 ⁻⁴
4	89378267	89427319	HERC5	89132710	5.77x10 ⁻³
5	17130137	17217156	AC091878.1	16950494	1.59x10 ⁻⁴
5	17130137	17217156	AC091878.1	17147134	7.32x10 ⁻³
5	171760502	171881527	SH3PXD2B	172131183	3.02x10 ⁻³
5	172195092	172198203	DUSP1	172131183	3.02x10 ⁻³
5	172195092	172198203	DUSP1	172385451	5.69x10 ⁻³
5	176921996	176930648	RP11-1334A24.6	176759081	9.88x10 ⁻³
5	176921996	176930648	RP11-1334A24.6	176759115	9.71x10 ⁻³
5	176921996	176930648	RP11-1334A24.6	176789620	5.54x10 ⁻³
5	176928905	176937427	DOK3	176832034	9.25x10 ⁻³
5	176928905	176937427	DOK3	176846745	5.16x10 ⁻³

5	176928905	176937427	DOK3	176859147	9.23x10 ⁻³
5	178537851	178772431	ADAMTS2	178913356	9.18x10 ⁻³
6	49572889	49604587	RHAG	49493945	8.98x10 ⁻³
6	49695091	49712150	CRISP3	49493945	8.98x10 ⁻³
7	1127723	1133451	GPER	1095452	4.51x10 ⁻³
7	1127723	1133451	GPER	1338332	3.93x10 ⁻³
7	41728600	41742706	INHBA	41502683	8.89x10 ⁻³
7	48211056	48687091	ABCA13	48231093	8.56x10 ⁻³
7	101459183	101901513	CUX1	101264700	5.74x10 ⁻⁴
7	101459183	101901513	CUX1	101335114	3.86x10 ⁻³
7	101459183	101901513	CUX1	101365760	3.77x10 ⁻³
7	101459183	101901513	CUX1	101927584	9.25x10 ⁻³
7	101459183	101901513	CUX1	102043849	6.68x10 ⁻³
8	133879204	134147143	TG	134106571	9.62x10 ⁻³
8	133879204	134147143	TG	134135662	4.07x10 ⁻³
8	133879204	134147143	TG	134251022	4.62x10 ⁻³
9	34398181	34458568	FAM219A	34181255	8.11x10 ⁻³
9	34398181	34458568	FAM219A	34490485	7.13x10 ⁻³
9	39072763	39288300	CNTNAP3	39033093	9.08x10 ⁻³
9	95473644	95527083	BICD2	95233776	8.09x10 ⁻³
9	95473644	95527083	BICD2	95413555	2.59x10 ⁻³
9	132250938	132275965	LINC00963	132109786	5.17x10 ⁻³
9	132250938	132275965	LINC00963	132109934	8.85x10 ⁻³
9	132250938	132275965	LINC00963	132257756	7.62x10 ⁻⁴
9	132250938	132275965	LINC00963	132357588	4.05x10 ⁻³
9	136028334	136039332	GBGT1	136181762	9.36x10 ⁻³
10	6186842	6277507	PFKFB3	6018769	7.86x10 ⁻³
10	45940018	45948569	RP11-67C2.2	45817319	2.22x10 ⁻⁴
10	45940018	45948569	RP11-67C2.2	45870144	2.69x10 ⁻⁴
10	62538088	62546827	CDK1	62751435	8.54x10 ⁻³
10	94352824	94415152	KIF11	94336562	3.24x10 ⁻³
10	94352824	94415152	KIF11	94550862	5.01x10 ⁻³
10	95256368	95288849	CEP55	95051132	2.50x10 ⁻³
10	95256368	95288849	CEP55	95062681	7.38x10 ⁻³
10	95256368	95288849	CEP55	95327878	7.25x10 ⁻³
10	99473464	99477909	MARVELD1	99258396	9.21x10 ⁻³
10	99473464	99477909	MARVELD1	99446317	4.06x10 ⁻³
10	105791045	105845638	COL17A1	105801896	9.89x10 ⁻³
11	45950869	46142985	PHF21A	45803411	4.33x10 ⁻³
11	76839309	76926286	MYO7A	76796073	7.66x10 ⁻³
11	76839309	76926286	MYO7A	76900467	1.02x10 ⁻³
11	94277016	94283064	FUT4	94502805	6.06x10 ⁻³
11	94300473	94354587	PIWIL4	94502805	6.06x10 ⁻³
12	2966846	2986321	FOXM1	3053621	8.55x10 ⁻³
12	8071823	8088892	SLC2A3	7910506	7.00x10 ⁻³
12	8071823	8088892	SLC2A3	7979933	1.96x10 ⁻³
12	8071823	8088892	SLC2A3	8070526	7.36x10 ⁻³

12	10310898	10324790	OLR1	10362476	3.37x10 ⁻³
12	12482217	12503169	MANSC1	12388557	8.78x10 ⁻³
12	53662082	53687427	ESPL1	53660942	6.75x10 ⁻⁴
12	109185694	109251359	SSH1	109170831	3.43x10 ⁻³
12	120123594	120315095	CIT	120398191	8.51x10 ⁻³
12	120123594	120315095	CIT	120549925	8.00x10 ⁻³
13	28577410	28674729	FLT3	28368126	9.70x10 ⁻³
13	28577410	28674729	FLT3	28503059	1.07x10 ⁻³
13	28577410	28674729	FLT3	28659295	4.69x10 ⁻³
14	23242431	23285101	SLC7A7	23310733	4.64x10 ⁻³
14	23305741	23316808	MMP14	23310733	4.64x10 ⁻³
14	23415436	23426351	HAUS4	23310733	4.64x10 ⁻³
14	25042723	25045466	CTSG	24804985	9.50x10 ⁻³
14	55614833	55658396	DLGAP5	55584030	4.28x10 ⁻³
14	77490885	77495042	IRF2BPL	77334528	5.90x10 ⁻³
14	77490885	77495042	IRF2BPL	77341636	8.06x10 ⁻³
14	95648275	95786245	CLMN	95983475	4.06x10 ⁻³
14	95648275	95786245	CLMN	96033927	6.55x10 ⁻⁴
14	102829299	102968818	TECPR2	102776206	3.45x10 ⁻³
14	102829299	102968818	TECPR2	102781393	8.67x10 ⁻³
14	102829299	102968818	TECPR2	103005143	4.60x10 ⁻³
14	102829299	102968818	TECPR2	103097135	6.38x10 ⁻³
14	102829299	102968818	TECPR2	103160813	9.79x10 ⁻³
15	40380091	40398639	BMF	40544713	6.33x10 ⁻³
15	40380091	40398639	BMF	40559641	9.19x10 ⁻³
15	40886446	40954881	CASC5	41150887	8.20x10 ⁻³
15	40987326	41024356	RAD51	41150887	8.20x10 ⁻³
16	3082482	3089134	RP11-473M20.5	2840498	5.84x10 ⁻³
16	3082482	3089134	RP11-473M20.5	3011066	8.47x10 ⁻³
16	3082482	3089134	RP11-473M20.5	3065902	2.72x10 ⁻³
16	3101992	3109364	RP11-473M20.7	3236725	9.36x10 ⁻³
16	3101992	3109364	RP11-473M20.7	3239683	5.22x10 ⁻³
16	27325229	27376099	IL4R	27367633	1.35x10 ⁻³
16	31271287	31344213	ITGAM	31540544	7.98x10 ⁻³
16	67207755	67209640	NOL3	67195610	2.60x10 ⁻³
17	9813925	9929623	GAS7	9891114	1.80x10 ⁻³
17	38544772	38574202	TOP2A	38584962	3.21x10 ⁻³
17	38544772	38574202	TOP2A	38755761	8.44x10 ⁻³
17	40351194	40428424	STAT5B	40192921	4.43x10 ⁻³
17	40351194	40428424	STAT5B	40266545	1.77x10 ⁻³
17	56347216	56358296	MPO	56268785	7.75x10 ⁻³
17	56347216	56358296	MPO	56405141	6.24x10 ⁻³
17	76419777	76573476	DNAH17	76373256	5.16x10 ⁻³
17	76422409	76422834	AC061992.1	76373256	5.16x10 ⁻³
17	79008946	79091232	BAIAP2	79067113	3.14x10 ⁻³
17	79091095	79139872	AATK	79097160	8.14x10 ⁻³
17	79091095	79139872	AATK	79163584	8.63x10 ⁻³

17	79276623	79283048	LINC00482	79163584	8.63x10 ⁻³
17	79276623	79283048	LINC00482	79350157	3.52x10 ⁻³
17	79276623	79283048	LINC00482	79433743	7.86x10 ⁻³
17	79276623	79283048	LINC00482	79450592	7.80x10 ⁻⁴
18	657603	673499	TYMS	559877	8.32x10 ⁻³
18	657603	673499	TYMS	904650	4.31x10 ⁻³
18	61582744	61602476	SERPINB10	61559787	4.73x10 ⁻³
19	827830	832017	AZU1	581656	5.43x10 ⁻³
19	827830	832017	AZU1	770078	9.66x10 ⁻³
19	827830	832017	AZU1	788944	8.25x10 ⁻³
19	827830	832017	AZU1	788951	8.07x10 ⁻³
19	827830	832017	AZU1	808617	1.76x10 ⁻³
19	827830	832017	AZU1	823534	4.37x10 ⁻³
19	827830	832017	AZU1	835209	1.61x10 ⁻³
19	827830	832017	AZU1	928287	2.21x10 ⁻³
19	827830	832017	AZU1	999969	5.73x10 ⁻³
19	827830	832017	AZU1	1036519	6.03x10 ⁻³
19	827830	832017	AZU1	1060664	3.30x10 ⁻³
19	827830	832017	AZU1	1079683	1.73x10 ⁻³
19	827830	832017	AZU1	1079726	8.22x10 ⁻³
19	827830	832017	AZU1	1079743	7.55x10 ⁻³
19	827830	832017	AZU1	1079745	9.42x10 ⁻³
19	827830	832017	AZU1	1079751	9.46x10 ⁻³
19	5993174	6110664	RFX2	5823791	4.74x10 ⁻³
19	5993174	6110664	RFX2	6273928	3.29x10 ⁻⁴
19	5993174	6110664	RFX2	6274810	4.50x10 ⁻³
19	11257830	11266484	SPC24	11221291	9.46x10 ⁻³
19	11257830	11266484	SPC24	11285276	9.11x10 ⁻³
19	11257830	11266484	SPC24	11367635	7.42x10 ⁻³
19	11257830	11266484	SPC24	11492648	6.28x10 ⁻³
19	35531409	35557477	HPN	35490410	6.66x10 ⁻³
19	35531409	35557477	HPN	35514655	6.11x10 ⁻⁵
19	35531409	35557477	HPN	35514678	6.56x10 ⁻³
19	35531409	35557477	HPN	35514694	8.94x10 ⁻³
19	35531409	35557477	HPN	35569572	5.49x10 ⁻³
19	35531409	35557477	HPN	35610338	6.75x10 ⁻³
19	39805291	39811498	CTC-246B18.8	39575128	8.90x10 ⁻⁵
19	39805291	39811498	CTC-246B18.8	39589635	5.93x10 ⁻³
19	42259427	42276113	CEACAM6	42416578	5.05x10 ⁻⁴
19	52800421	52829180	ZNF480	52956986	7.69x10 ⁻³
19	54296854	54327657	NLRP12	54218164	4.68x10 ⁻³
19	54296854	54327657	NLRP12	54266550	5.24x10 ⁻³
19	54296854	54327657	NLRP12	54545252	2.96x10 ⁻³
19	54573200	54584634	TARM1	54545252	2.96x10 ⁻³
19	54573200	54584634	TARM1	54607111	3.44x10 ⁻³
19	55824168	55836708	TMEM150B	55591996	2.24x10 ⁻³
19	55824168	55836708	TMEM150B	55760810	6.97x10 ⁻³

20	1784662	1798252	RP5-968J1.1	1876682	7.03x10 ⁻³
20	1874812	1920540	SIRPA	1920583	4.29x10 ⁻³
20	4760669	4804291	RASSF2	4969742	4.66x10 ⁻³
20	36932551	36965905	BPI	36853042	3.85x10 ⁻³
20	48807119	48809227	CEBPB	48572573	1.61x10 ⁻³
20	48807119	48809227	CEBPB	48692927	8.98x10 ⁻³
21	34638664	34669539	IL10RB	34399336	7.39x10 ⁻³
21	34638664	34669539	IL10RB	34436976	5.55x10 ⁻³
21	34638664	34669539	IL10RB	34436978	4.69x10 ⁻³
21	34638664	34669539	IL10RB	34850937	6.38x10 ⁻³
21	35014783	35210802	ITSN1	34850937	6.38x10 ⁻³
21	35014783	35210802	ITSN1	34976656	1.07x10 ⁻³
21	35014783	35210802	ITSN1	35219554	9.97x10 ⁻³
21	39751949	39956869	ERG	39840765	9.10x10 ⁻³
22	19467348	19508135	CDC45	19701472	6.40x10 ⁻³
22	23401593	23484241	RTDR1	23362153	9.35x10 ⁻³
22	23401593	23484241	RTDR1	23644647	6.97x10 ⁻³
X	77526968	77583188	CYSLTR1	77359794	8.10x10 ⁻³

Table IV. Results of the detailed reactome pathway analysis of 14 cell cycle genes. Pathways are sorted by the P-value.

Pathway name	Entities found	Entities total	Entities ratio	Entities P-value	Entities FDR	Reactions found	Reactions total	Reactions ratio	Submitted entities found
Cell Cycle	9	574	0.059	3.25x10 ⁻⁸	9.88x10 ⁻⁶	89	345	0.046	SPC24; ESPL1; CLSPN; CDC45; CENPF; FOXM1; CDK1; CENPF; RAD51
Cell Cycle, Mitotic	7	496	0.051	4.12x10 ⁻⁶	6.02x10 ⁻⁴	84	272	0.036	SPC24; ESPL1; CDC45; CENPF; FOXM1; CDK1; CENPF
Polo-like kinase mediated events	3	23	0.002	5.97x10 ⁻⁶	6.02x10 ⁻⁴	12	15	0.002	CENPF; FOXM1; CENPF
G2/M Transition	4	133	0.014	4.30x10 ⁻⁵	0.002	47	62	0.008	CENPF; FOXM1; CDK1; CENPF
Mitotic G2-G2/M phases	4	135	0.014	4.56x10 ⁻⁵	0.002	47	64	0.009	CENPF; FOXM1; CDK1; CENPF
G2/M Checkpoints	3	46	0.005	4.67x10 ⁻⁵	0.002	4	16	0.002	CLSPN; CDC45; CDK1
G1/S-Specific Transcription	2	17	0.002	3.19x10 ⁻⁴	0.014	1	1	1.33x10 ⁻⁴	CDC45; CDK1
Cyclin A/B1 associated events during G2/M transition	2	26	0.003	7.39x10 ⁻⁴	0.024	21	24	0.003	FOXM1; CDK1
Cell Cycle Checkpoints	3	121	0.012	7.93x10 ⁻⁴	0.024	4	38	0.005	CLSPN; CDC45; CDK1
Resolution of Sister Chromatid Cohesion	3	122	0.013	8.12x10 ⁻⁴	0.024	5	8	0.001	SPC24; CENPF; CDK1
Mitotic Prometaphase	3	130	0.013	9.75x10 ⁻⁴	0.026	7	13	0.002	SPC24; CENPF; CDK1
M Phase	4	306	0.032	0.001	0.026	19	63	0.008	SPC24; ESPL1; CENPF; CDK1
E2F mediated regulation of DNA replication	2	33	0.003	0.001	0.027	3	6	7.99x10 ⁻⁴	CDC45; CDK1
Activation of ATR in response to replication stress	2	39	0.004	0.002	0.032	2	9	0.001	CLSPN; CDC45
Kinesins	2	44	0.005	0.002	0.032	4	14	0.002	KIF15; KIF11
Separation of Sister Chromatids	3	179	0.018	0.002	0.032	4	8	0.001	SPC24; ESPL1; CENPF
Mitotic Anaphase	3	193	0.020	0.003	0.032	4	11	0.001	SPC24; ESPL1; CENPF
Mitotic Metaphase and Anaphase	3	194	0.020	0.003	0.032	4	12	0.002	SPC24; ESPL1; CENPF
Assembly of the RAD51-ssDNA nucleoprotein complex	1	5	5.16x10 ⁻⁴	0.008	0.032	3	3	3.99x10 ⁻⁴	RAD51
Phosphorylation of proteins involved in the G2/M transition by Cyclin A:Cdc2 complexes	1	5	5.16x10 ⁻⁴	0.008	0.032	2	2	2.66x10 ⁻⁴	CDK1

Presynaptic phase of homologous DNA pairing and strand exchange	1	6	6.20×10^{-4}	0.009	0.032	4	7	9.32×10^{-4}	RAD51
G2/M DNA replication checkpoint	1	7	7.23×10^{-4}	0.011	0.032	2	2	2.66×10^{-4}	CDK1
Homologous DNA pairing and strand exchange	1	7	7.23×10^{-4}	0.011	0.032	4	8	0.001	RAD51
Chk1/Chk2(Cds1) mediated inactivation of Cyclin B:Cdk1 complex	1	7	7.23×10^{-4}	0.011	0.032	1	5	6.66×10^{-4}	CDK1
Phosphorylation of Emi1	1	8	8.26×10^{-4}	0.012	0.032	1	2	2.66×10^{-4}	CDK1
G1/S Transition	2	113	0.012	0.013	0.032	7	32	0.004	CDC45; CDK1
Cyclin B2 mediated events	1	9	9.29×10^{-4}	0.014	0.032	2	2	2.66×10^{-4}	CDK1
Activation of NIMA Kinases NEK9, NEK6, NEK7	1	9	9.29×10^{-4}	0.014	0.032	1	4	5.33×10^{-4}	CDK1
E2F-enabled inhibition of pre-replication complex formation	1	10	0.001	0.015	0.032	2	2	2.66×10^{-4}	CDK1
Unwinding of DNA	1	11	0.001	0.017	0.032	1	4	5.33×10^{-4}	CDC45
G2/M DNA damage checkpoint	1	11	0.001	0.017	0.032	1	7	9.32×10^{-4}	CDK1
MHC class II antigen presentation	2	135	0.014	0.018	0.032	1	23	0.003	KIF15; KIF11
MASTL Facilitates Mitotic Progression	1	12	0.001	0.018	0.032	1	4	5.33×10^{-4}	CDK1
Mitotic G1-G1/S phases	2	139	0.014	0.019	0.032	8	53	0.007	CDC45; CDK1
ERK1 activation	1	13	0.001	0.020	0.032	1	6	7.99×10^{-4}	CDK1
Factors involved in megakaryocyte development and platelet production	2	150	0.015	0.022	0.032	4	42	0.006	KIF15; KIF11
Condensation of Prometaphase Chromosomes	1	15	0.002	0.023	0.032	1	4	5.33×10^{-4}	CDK1
ERK activation	1	15	0.002	0.023	0.032	1	11	0.001	CDK1
Phosphorylation of the APC/C	1	17	0.002	0.026	0.032	1	2	2.66×10^{-4}	CDK1
Golgi Cisternae Pericentriolar Stack Reorganization	1	17	0.002	0.026	0.032	1	6	7.99×10^{-4}	CDK1
Homologous recombination repair of replication-independent double-strand breaks	1	19	0.002	0.029	0.032	4	24	0.003	RAD51
Homologous Recombination Repair	1	19	0.002	0.029	0.032	4	24	0.003	RAD51
APC/C:Cdc20 mediated degradation of Cyclin B	1	21	0.002	0.032	0.032	3	3	3.99×10^{-4}	CDK1
RAF/MAP kinase cascade	1	21	0.002	0.032	0.032	1	19	0.003	CDK1

Depolymerisation of the Nuclear Lamina	1	23	0.002	0.035	0.035	2	6	7.99×10^{-4}	CDK1
Double-Strand Break Repair	1	25	0.003	0.038	0.038	4	32	0.004	RAD51
SOS-mediated signalling	1	26	0.003	0.040	0.040	1	21	0.003	CDK1
GRB2 events in EGFR signaling	1	26	0.003	0.040	0.040	1	22	0.003	CDK1
Recruitment of NuMA to mitotic centrosomes	1	27	0.003	0.041	0.041	1	3	3.99×10^{-4}	CDK1
G0 and Early G1	1	27	0.003	0.041	0.041	1	10	0.001	CDK1
SHC-mediated signalling	1	27	0.003	0.041	0.041	1	21	0.003	CDK1
SHC1 events in EGFR signaling	1	27	0.003	0.041	0.041	1	23	0.003	CDK1
Signalling to p38 via RIT and RIN	1	28	0.003	0.042	0.042	1	22	0.003	CDK1
ARMS-mediated activation	1	29	0.003	0.044	0.044	1	24	0.003	CDK1
SHC-related events	1	30	0.003	0.045	0.045	1	24	0.003	CDK1
Signaling by Leptin	1	30	0.003	0.045	0.045	1	38	0.005	CDK1
Frs2-mediated activation	1	32	0.003	0.048	0.048	1	25	0.003	CDK1
Activation of the pre-replicative complex	1	33	0.003	0.050	0.050	4	8	0.001	CDC45
SHC-related events triggered by IGF1R	1	33	0.003	0.050	0.050	1	23	0.003	CDK1

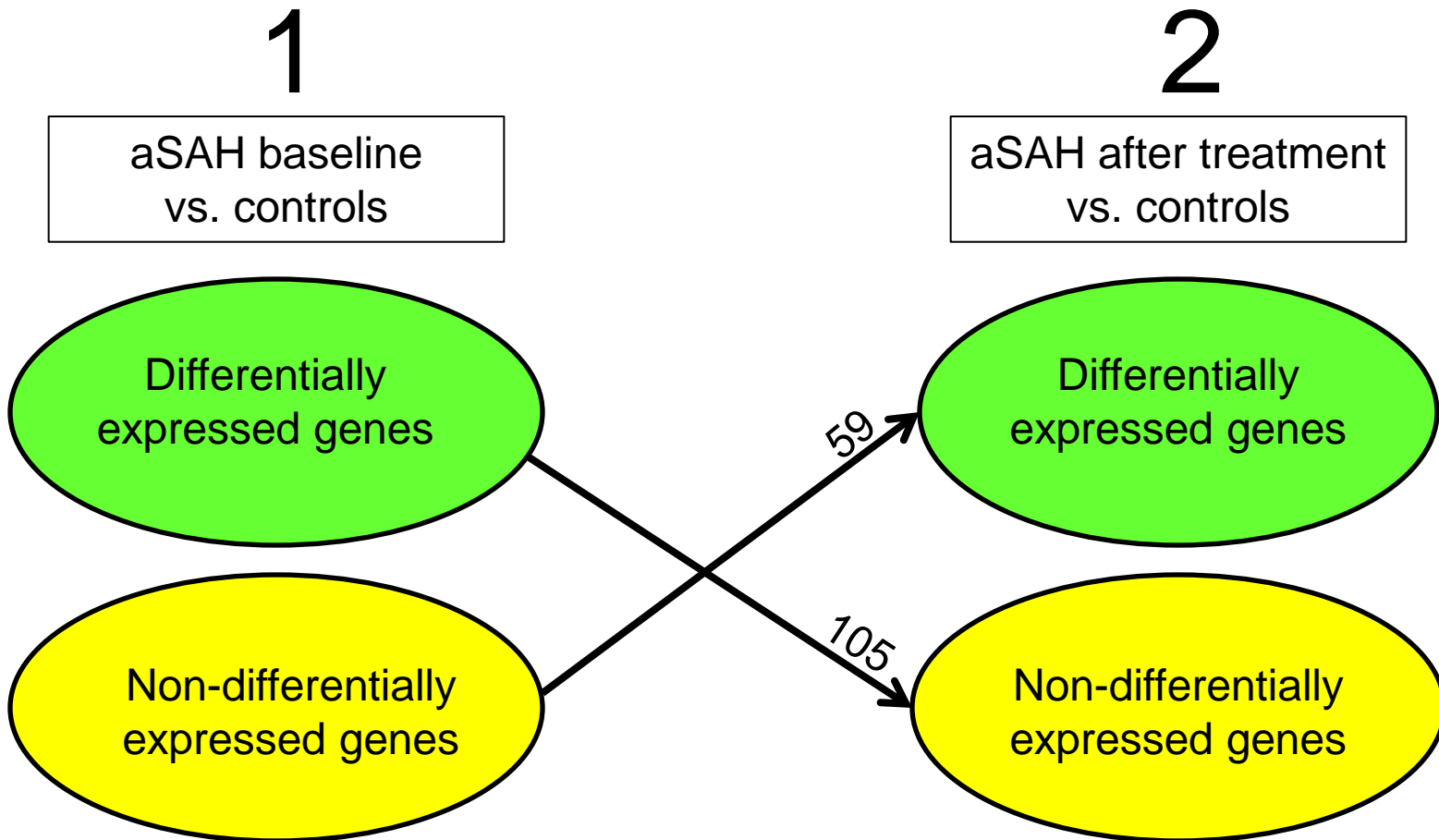


Figure I. Schematic overview of the analysis of the 451 differentially expressed (DE) genes using the controls who did not receive the treatment. We subsequently focused on the 164 genes that changed the DE status between the two analyses.

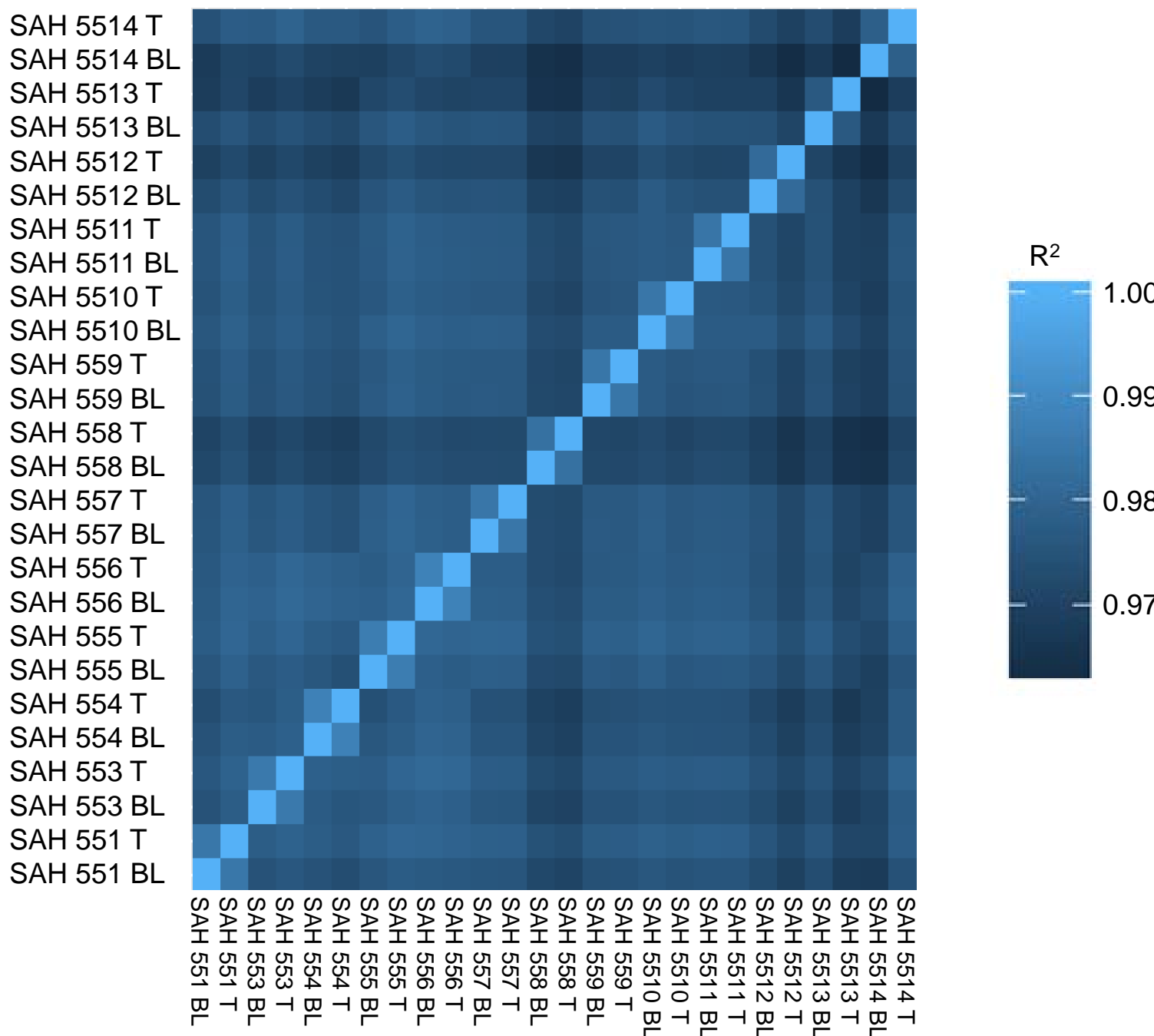


Figure II. The correlation of 676,543 CpG sites assayed in all individuals between the samples. BL indicates baseline and T indicates treatment. The overall methylation status changed very little within an individual (~98%) and between the individuals (~97.5%).

Remote Ischemic Conditioning Alters Methylation and Expression of Cell Cycle Genes in Aneurysmal Subarachnoid Hemorrhage

Elina Nikkola, Azim Laiwalla, Arthur Ko, Marcus Alvarez, Mark Connolly, Yinn Cher Ooi, William Hsu, Alex Bui, Päivi Pajukanta and Nestor R. Gonzalez

Stroke. 2015;46:2445-2451; originally published online August 6, 2015;
doi: 10.1161/STROKEAHA.115.009618

Stroke is published by the American Heart Association, 7272 Greenville Avenue, Dallas, TX 75231
Copyright © 2015 American Heart Association, Inc. All rights reserved.
Print ISSN: 0039-2499. Online ISSN: 1524-4628

The online version of this article, along with updated information and services, is located on the World Wide Web at:

<http://stroke.ahajournals.org/content/46/9/2445>

Data Supplement (unedited) at:

<http://stroke.ahajournals.org/content/suppl/2015/08/07/STROKEAHA.115.009618.DC1.html>

Permissions: Requests for permissions to reproduce figures, tables, or portions of articles originally published in *Stroke* can be obtained via RightsLink, a service of the Copyright Clearance Center, not the Editorial Office. Once the online version of the published article for which permission is being requested is located, click Request Permissions in the middle column of the Web page under Services. Further information about this process is available in the [Permissions and Rights Question and Answer](#) document.

Reprints: Information about reprints can be found online at:
<http://www.lww.com/reprints>

Subscriptions: Information about subscribing to *Stroke* is online at:
<http://stroke.ahajournals.org//subscriptions/>